

Yu-Shiba-Rusinov bound states boost odd-frequency superconductivity

Subhajit Pal and Colin Benjamin*

*School of Physical Sciences, National Institute of Science Education & Research,
An OCC of Homi Bhabha National Institute, Jatni-752050, India*

We predict multi-fold amplification of odd-frequency superconducting pairing due to the emergence of zero energy Yu-Shiba-Rusinov bound states. We consider two setups; first, a metal-spin flipper-metal- s -wave superconductor (N_1 -sf- N_2 -S) junction, and second a superconductor-metal-spin flipper-metal-superconductor (S- N_1 -sf- N_2 -S) junction. We find that in the case of N_1 -sf- N_2 -S junction occurrence of zero energy Yu-Shiba-Rusinov bound states are accompanied by odd-frequency pairing, which is much larger than even frequency pairing. However, when zero energy Yu-Shiba-Rusinov bound states are absent, even frequency pairing dominates odd-frequency pairing. For S- N_1 -sf- N_2 -S junction, when zero energy Yu-Shiba-Rusinov bound states emerge, there is a $0 - \pi$ junction transition, and again odd-frequency pairing is much larger than even frequency pairing. Our results may help detect signatures of Yu-Shiba-Rusinov bound states via odd-frequency pairing and better understand the link.

I. INTRODUCTION

Odd-frequency superconductivity indicates a sign change in Cooper pair wavefunctions or pair amplitudes when the time coordinates of two electrons are interchanged. Generally, electron pairing occurs between electrons at equal times, which is classified as even frequency superconductivity. An even frequency Cooper pair can be further classified as an even frequency spin-singlet (Even-SS) pairing state or even frequency spin-triplet (Even-ST) pairing state. Examples of Even-SS pairing are s and d wave pairing, while the example of Even-ST pairing is p wave pairing[1]. As noted in the beginning, pairing may also happen at various times or at nonzero frequency, which was initially discovered in ^3He [2]. An odd-frequency Cooper pair can be either in an odd-frequency spin-singlet (Odd-SS) state or an odd-frequency spin-triplet (Odd-ST) state. A spin-triplet state, regardless of whether its even or odd frequency, can be either mixed spin-triplet(MST), i.e., $|\uparrow\downarrow\rangle + |\downarrow\uparrow\rangle$ or equal spin-triplet(EST), i.e., $|\uparrow\uparrow\rangle, |\downarrow\downarrow\rangle$. Spin singlet(SS) state is of one type alone, i.e., $|\uparrow\downarrow\rangle - |\downarrow\uparrow\rangle$. In Ref. [3], it has been shown that a spin flipper (magnetic impurity) at a metal- s -wave superconductor interface induces odd-frequency equal spin-triplet (Odd-EST) pairing[3]. Magnetic impurities may also induce bound states in s -wave superconductors, whose energies lie in the superconducting gap. This was first noted by Yu, Shiba, and Rusinov in the late 1960s and is now called the Yu-Shiba-Rusinov (YSR) state[4–6]. The interaction of Andreev reflected electrons or holes with impurity spin gives rise to these YSR states, see Refs. [7–9]. YSR bound states have been reported experimentally via scanning tunneling spectroscopy on superconducting Pb and Nb surfaces[10–12].

In this work, our primary motivation is to understand if there exists any link between odd-frequency pairing and YSR-bound states. We notice that for parameter regimes wherein zero energy YSR bound states appear, odd-frequency pairing dominates over even frequency pairing. However, for parameter regimes wherein zero energy YSR bound states are absent, even frequency pairing dominates over odd-frequency pairing. An enhancement of odd-frequency pairing due to YSR-bound states implies a nontrivial link between these remarkable effects. Furthermore, the odd-frequency superconductivity generated in our setups is equal to spin-triplet pairing due to interface Andreev scattering. Odd frequency mixed spin-triplet (Odd-MST) pairing[13] has also been reported in the vicinity of magnetic impurity.

EST pairing, unlike MST pairing, has significant implications for superconducting spintronics as spin is much more resilient to dephasing. In this paper, when zero energy YSR bound states appear, Odd-EST pairing dominates Even-EST pairing, while Odd-MST pairing and Even-MST pairings vanish. EST pairing supports dissipationless pure spin current, which has applications in superconducting spintronics[14, 15]. Further, via inducing Odd-EST pairing, one can effectively tune an even ω s -wave superconductor to an odd ω p -wave superconductor. YSR bound states are also important as they give false positives for Majorana bound states in chains of magnetic adatoms on superconductor[16].

The paper's organization is as follows: in the next section, we first present the two setups and discuss the theoretical background to our study by writing the Hamiltonian, wave functions, and boundary conditions required to calculate YSR bound states Josephson current and Green's functions. In the same section, we also discuss the procedure to calculate YSR bound states, Josephson current, and induced pairing amplitude from retarded Green's functions. Section

* colin.nano@gmail.com

III presents our results and explains the relation between odd-frequency pairing and YSR bound states in metal-spin flipper-metal-superconductor junction and superconductor-metal-spin flipper-metal-superconductor junction. In analysis, section IV, we discuss our results via a table. This paper is accompanied by a supplementary material[17] where we present Hamiltonian wavefunctions and boundary conditions for our two setups, discuss the procedure to form the retarded Green's functions for our models, and also provide the explicit form of expressions for anomalous Green's functions. Finally, we conclude in Section V.

II. THEORY

A. YSR bound states in metal-Superconductor and Superconductor-metal-Superconductor junctions with spin flipper

1. Hamiltonian

We choose two setups: (a) 1D metal (N)-metal (N)- s -wave superconductor (S) junction with a spin-flipper (sf) between the two metals as depicted in Fig. 1(a) and (b) two metals with an embedded spin-flipper between two s -wave superconductors as shown in Fig. 1(b). We use the BTK approach[18] to solve the problem. Spin-flipper is a δ -like magnetic impurity. The Hamiltonian for spin-flipper is[7, 19–22]:

$$H_{\text{spin-flipper}} = -\mathcal{J}_0\delta(x)\vec{s}\cdot\vec{S} \quad (1)$$

The model Hamiltonian in Bogoliubov-de Gennes (BdG) formalism for metal-spin-flipper-metal-superconductor (N_1 -sf- N_2 -S) junction as shown in Fig. 1(a) is given by,

$$H_{BdG}^{N_1\text{-sf-}N_2\text{-S}}(x) = \begin{pmatrix} H_M\hat{I} & i\Delta\theta(x)\hat{\sigma}_y \\ -i\Delta^*\theta(x)\hat{\sigma}_y & -H_M\hat{I} \end{pmatrix}, \quad (2)$$

where $H_M = p^2/2m^* + V\delta(x) - \mathcal{J}_0\delta(x+a)\vec{s}\cdot\vec{S} - E_F$, $\theta(x)$ is the Heaviside step function, Δ is the gap parameter for s -wave superconductor. $\frac{p^2}{2m^*}$ is electron's kinetic energy with effective mass m^* , V is strength of the δ -type potential barrier at the interface between metal and superconductor, the third term represents the exchange coupling of strength \mathcal{J}_0 between electron's spin (\vec{s}) and spin (\vec{S}) of spin flipper, \hat{I} is an unit matrix, $\hat{\sigma}$ represents the Pauli matrices and E_F denotes the Fermi energy. In this paper, the dimensionless parameter $\mathcal{J} = \frac{m^*\mathcal{J}_0}{k_F}$ is used as a measure of strength of exchange coupling[19] and $Z = \frac{m^*V}{\hbar^2k_F}$ as a measure of interface transparency[18].

The model Hamiltonian in BdG formalism for superconductor-metal-spin-flipper-metal-superconductor (S- N_1 -sf- N_2 -S) junction as shown in Fig. 1(b) is given below,

$$H_{BdG}^{S\text{-}N_1\text{-sf-}N_2\text{-S}}(x) = \begin{pmatrix} H_J\hat{I} & i\Delta_J\hat{\sigma}_y \\ -i\Delta_J^*\hat{\sigma}_y & -H_J\hat{I} \end{pmatrix}, \quad (3)$$

where $H_J = p^2/2m^* + V[\delta(x+a/2) + \delta(x-a/2)] - J_0\delta(x)\vec{s}\cdot\vec{S} - E_F$. The superconducting gap Δ_J is of the form $\Delta_J = \Delta[e^{i\varphi_L}\Theta(-x-a/2) + e^{i\varphi_R}\Theta(x-a/2)]$. φ_L and φ_R are the superconducting phases for left and right superconductors respectively. The wavefunctions and boundary conditions of our chosen setups are provided in supplementary material[17].

2. YSR bound states in metal-spin flipper-metal-Superconductor junction

To calculate YSR bound states for this case, we first compute differential charge conductance using the well-established definitions as[23, 24]

$$\mathcal{G}_c = \mathcal{G}_N(1 + \mathcal{A}_{11} + \mathcal{A}_{12} - \mathcal{B}_{11} - \mathcal{B}_{12}), \quad (4)$$

where $\mathcal{G}_N = 2e^2/h$ is the charge conductance when a metallic region replaces the superconducting region in our model with $\Delta = 0$. \mathcal{A}_{11} is the Andreev reflection probability when a spin-up electron is reflected as a spin-up hole, \mathcal{A}_{12} is the Andreev reflection probability when a spin-up electron is reflected back as a spin down hole, \mathcal{B}_{11} is the normal reflection probability when a spin-up electron is reflected as a spin-up electron and, finally \mathcal{B}_{12} is the normal reflection

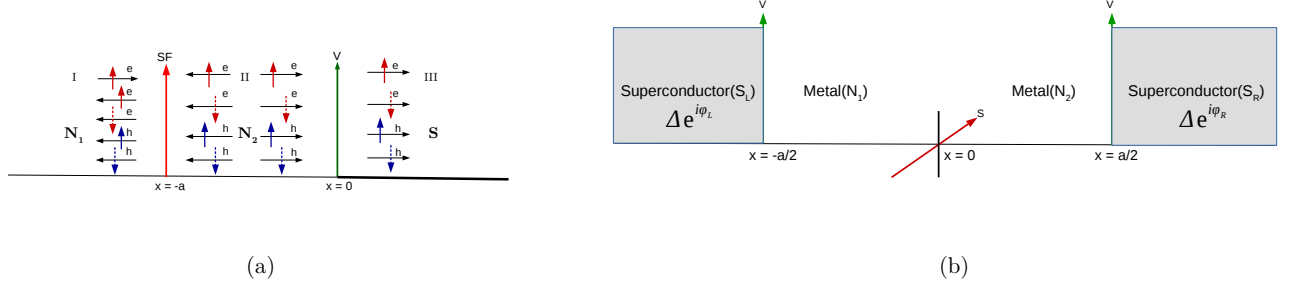


FIG. 1: (a) N_1N_2S junction with spin flipper at N_1N_2 interface and a δ -like potential barrier at N_2S interface. The scattering of a spin up electron incident is shown, (b) Josephson junction composed of two metals and a spin flipper with spin S and magnetic moment m' at $x = 0$ embedded between two s -wave superconductors.

probability when a spin-up electron is reflected as a spin-down electron, see supplementary material[17] for calculation of these reflection probabilities. From complex poles of differential charge conductance \mathcal{G}_c in Eq. (4), we can get energy bound states E^\pm . The real part of the poles is the energy where YSR peaks appear, while the imaginary part of the poles denotes the width of the peaks.

In Figs. 2(a), (b) we plot YSR bound states as a function of interface transparency Z for two cases: (a) when zero energy YSR states appear and (b) when zero energy YSR states don't appear. From Fig. 2(a), we see that for high values of spin flipper's spin and low values of exchange interaction, two bound state energies merge at zero energy for some particular values of Z . For these values of Z , zero energy YSR bound states appear as conductance peaks in Fig. 2(c) which depicts a plot of normalized charge conductance as an energy function. However, for other values of spin flipper spin and exchange interaction, no mergers are seen, see Fig. 2(b), implying the absence of zero energy YSR bound states.

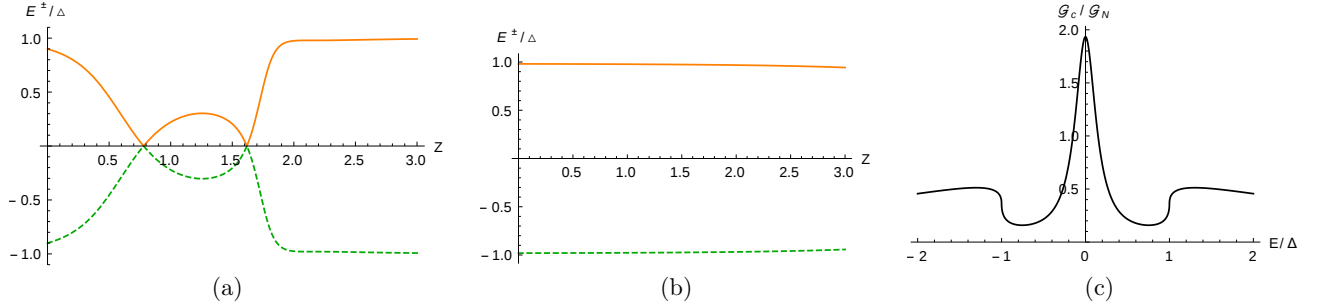


FIG. 2: Energy bound states vs Z for (a) when zero energy YSR bound states appear and for (b) when zero energy YSR bound states don't appear, (c) Normalized charge conductance vs E/Δ . Parameters: $S = \frac{19}{2}$ (for (a) and (c)), $S = \frac{9}{2}$ (for (b)), $\mathcal{F} = 10$ (for (a) and (c)), $\mathcal{F} = 5$ (for (b)), $\mathcal{J} = 0.4$ (for (a) and (c)), $\mathcal{J} = 2$ (for (b)), $Z = 0.78$ (for (c)), $k_F a = 0.8437\pi$ (for (a) and (c)), $k_F a = \pi$ (for (b)).

3. YSR bound states in superconductor-metal-spin-flipper-metal-superconductor junction

An electron in the metallic region is incident at the NS interface with an energy below the superconducting gap that cannot penetrate the superconductor. However, at the NS interface, Andreev's reflection may happen, in which a hole with opposite momentum is reflected into normal metal, and a Cooper pair is generated in the superconductor. The same effect is also present with an identical electron/hole combination at the SN interface. Therefore a bound state is formed between the two superconductors, an Andreev bound state. From Andreev bound states, one can calculate Free energy and Josephson current through the junction. The procedure to derive Andreev bound states is given in supplementary material. For our S-N-sf-N-S system we obtain Andreev bound states as $E_k(\varphi) = E_\sigma^\pm(\varphi) = \pm E_\sigma(\varphi)$,

($k = \{1, \dots, 4\}$, $\sigma = \uparrow, \downarrow$). Our work considers the short junction limit ($a \ll \xi$, where ξ is the superconducting coherence length). Thus total Josephson current is the same as the Josephson bound state current. The Josephson current can be calculated from Andreev energy bound states[25],

$$I = \frac{2e}{\hbar} \sum_k f(E_k) \frac{dE_k}{d\varphi} = -\frac{2e}{\hbar} \sum_\sigma \tanh\left(\frac{\beta E_\sigma}{2}\right) \frac{dE_\sigma}{d\varphi}. \quad (5)$$

In Figs. 3(a), (b), we plot Andreev energy bound states as a function of exchange interaction \mathcal{J} for high values of spin-flip probability of spin-flipper. From Fig. 3(a), we see that for $\mathcal{J} = 0.1267$, two bound state energies merge, and YSR bound states to occur; see also Ref. [9]. However, from Fig. 3(b), it is seen that for high values of \mathcal{J} , no merger is seen, indicating the absence of zero energy YSR bound states. In Fig. 3(c), we plot Josephson's current and its absolute value as a function of \mathcal{J} . We notice that for $\mathcal{J} = 0.1267$ when zero energy YSR bound states appear, there is a discontinuous change as a function of \mathcal{J} in Josephson current because of a $0 - \pi$ junction transition in which Josephson current changes its sign, marking the presence of a YSR state.

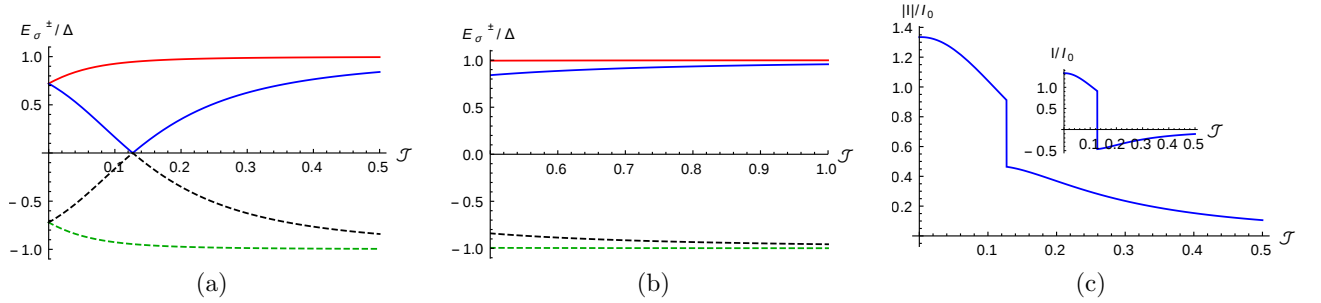


FIG. 3: (a) Energy bound states vs \mathcal{J} in presence of spin flip scattering, (b) Energy bound states vs \mathcal{J} in absence of spin flip scattering, (c) Josephson current and its absolute value vs \mathcal{J} . Parameters: $S = \frac{21}{2}$, $m' = -\frac{1}{2}$, $\mathcal{F} = 11$, $\varphi = \pi/2$, $Z = 0.1$, $k_F a = \pi$, $I_0 = e\Delta/\hbar$.

B. Retarded and Advanced Green's functions in the presence of YSR bound states

The main aim of our work is to check whether the presence of YSR-bound states has any bearing on the odd ω pairing generated. To this end we construct retarded Green's function $G^r(x, x', \omega)$ for our setups shown in Figs. 1(a) & (b) from the scattering processes at the interface[26]. We follow Refs. 27 and 28, and the retarded and advanced Green's function calculation are provided in the supplementary material[17]. Pairing amplitudes in our setup are calculated from retarded Green's function, as shown below.

1. Pairing amplitudes

The anomalous Green's function G_{eh}^r is defined as,

$$G_{eh}^r(x, x', \omega) = i \sum_{\mu=0}^3 f_\mu^r \sigma_\mu \sigma_2, \quad (6)$$

where σ_0 is a unit matrix, σ_μ ($\mu = 1, 2, 3$) represent the Pauli matrices. f_0^r represents SS ($\uparrow\downarrow - \downarrow\uparrow$), $f_{1,2}^r$ are the EST ($\downarrow\downarrow \pm \uparrow\uparrow$) and f_3^r corresponds to the MST ($\uparrow\downarrow + \downarrow\uparrow$) components of the pairing amplitude in Eq. 6. The EST components $\uparrow\uparrow$ and $\downarrow\downarrow$ are given by $f_{\uparrow\uparrow} = if_2^r - f_1^r$ and $f_{\downarrow\downarrow} = if_2^r + f_1^r$, respectively. Even and odd-frequency components are calculated from,

$$f_i^E(x, x', \omega) = \frac{1}{2} [f_i^r(x, x', \omega) + f_i^a(x, x', -\omega)], \text{ and } f_i^O(x, x', \omega) = \frac{1}{2} [f_i^r(x, x', \omega) - f_i^a(x, x', -\omega)], \quad (7)$$

f_i^a being the advanced Green's function and can be derived using[27] $G^a(x, x', \omega) = [G^r(x', x, \omega)]^\dagger$. The even and odd-frequency EST pairings can then be derived, see Eq. (7), as

$$\begin{aligned} f_{\uparrow\uparrow}^E &= if_2^E - f_1^E, & f_{\downarrow\downarrow}^E &= if_2^E + f_1^E, \\ f_{\uparrow\uparrow}^O &= if_2^O - f_1^O, & f_{\downarrow\downarrow}^O &= if_2^O + f_1^O. \end{aligned} \quad (8)$$

III. RESULTS

A. Odd-frequency pairing and YSR bound states in N_1 -SF- N_2 -S junction

1. Spin singlet superconducting pairing induced in N_1 -SF- N_2 -S junction

We compute induced even/odd-frequency superconducting pairing directly from anomalous components of $G^r(x, x', \omega)$ using Eqs. (6), (7) and (8). For spin singlet (SS) pairing we find,

$$\begin{aligned} f_0^E(x, x', \omega) &= \frac{\eta uv}{2i(u^2 - v^2)} e^{-\gamma|x-x'|} \left[\frac{e^{ik_F|x-x'|}}{q_e^S} + \frac{e^{-ik_F|x-x'|}}{q_h^S} \right] + \frac{\eta uv}{2i(u^2 - v^2)} e^{-\gamma(x+x')} \left[\frac{b_{51} e^{ik_F(x+x')}}{q_e^S} + \frac{b_{82} e^{-ik_F(x+x')}}{q_h^S} \right] \\ &\quad + \frac{\eta}{2i(u^2 - v^2)} e^{-\gamma(x+x')} \frac{a_{81} \cos[k_F(x - x')](k_F + i\gamma(u^2 - v^2))}{(k_F^2 + \gamma^2)}, \quad \text{for } x > 0 \end{aligned} \quad (9)$$

$$\text{and } f_0^O(x, x', \omega) = \frac{\eta a_{81}(k_F(u^2 - v^2) + i\gamma)}{2(u^2 - v^2)(k_F^2 + \gamma^2)} \sin[k_F(x - x')] e^{-\gamma(x+x')}, \quad \text{for } x > 0, \quad (10)$$

where $q^L = \frac{\omega k_F}{2E_F}$ and the normal (b_{51} , b_{82}) and Andreev reflection amplitudes (a_{12} , a_{81}) are calculated from the wavefunctions in Eq. (4) of supplementary material (SM), and imposing boundary conditions on these, see Eqs. (6,7) of SM. Here the normal and Andreev reflection amplitudes b_{51} mean normal reflection of incident spin up electronlike quasiparticle as a spin up electronlike quasiparticle, a_{12} mean Andreev reflection of incident spin up electron as a spin down hole, similarly b_{82} and a_{81} are defined, see SM (below Eq. (4)) for details. From Eq. (10) we see

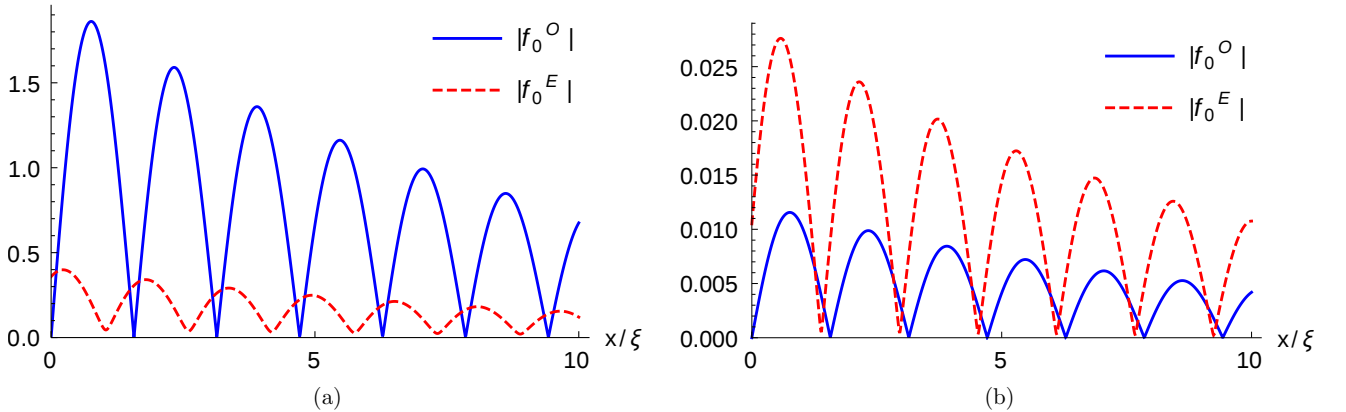


FIG. 4: The magnitudes of the Even-SS and Odd-SS pairings induced in the S region vs position x for (a) when zero energy YSR states are present, (b) when zero energy YSR states are absent. Parameters: $S = \frac{19}{2}$ (Fig. 4(a)), $S = \frac{9}{2}$ (Fig. 4(b)), $\mathcal{F} = \mathcal{F}' = 10$ (Fig. 4(a)), $\mathcal{F} = \mathcal{F}' = 5$ (Fig. 4(b)), $Z = 0.78$, $\mathcal{J} = 0.4$ (Fig. 4(a)), $\mathcal{J} = 2$ (Fig. 4(b)), $x' = 0$, $k_F a = 0.8437\pi$ (Fig. 4(a)), $k_F a = \pi$ (Fig. 4(b)), $\omega = 0$, $E_F = 10\Delta$.

that at $\omega = 0$, odd-SS pairing depends on $\sin[k_F(x - x')]e^{-\gamma(x+x')}$, therefore they exhibit an oscillatory decay with period $\frac{2\pi}{k_F}$ and decay length $\frac{1}{\gamma}$ where $\gamma = \sqrt{\Delta^2 - \omega^2[k_F/(2E_F)]}$. Even-SS and Odd-SS superconducting pairing in the superconducting region is plotted in Fig. 4. We consider two cases similar to Fig. 2. (a) when zero energy YSR states occur and (b) when zero energy YSR states are absent. From Fig. 4(a), we see that for high values of spin flipper spin and low values of exchange interaction \mathcal{J} , when zero energy YSR states appear (see Fig. 2(a)), Odd-SS pairing dominates Even-SS pairing. However, for low values of spin flipper spin and high values of exchange interaction, for

which zero energy YSR states are absent (see Fig. 2(b)), Even-SS dominates Odd-SS pairing, as shown in Fig. 4(b). We conclude that the multi-fold enhancement of odd-frequency spin-singlet superconducting pairing is, therefore, due to the occurrence of zero energy YSR states.

2. Spin triplet superconducting pairing induced in N_1 -SF- N_2 -S junction

ST pairing is two different types, EST and MST. However, we see MST pairing is absent and only EST pairing is finite since there is only spin flip scattering with vanishing spin mixing present in our setup (Fig. 1(a))[3]. For the Even-EST and Odd-EST superconducting pairing we get using Eq. (8),

$$f_{\uparrow\uparrow}^E(x, x', \omega) = -\frac{\eta a_{62}(k_F(u^2 - v^2) + i\gamma)}{2(u^2 - v^2)(k_F^2 + \gamma^2)} \sin[k_F(x - x')]e^{-\gamma(x+x')} = -f_{\downarrow\downarrow}^E(x, x', \omega), \quad \text{for } x > 0 \quad (11)$$

$$\begin{aligned} f_{\uparrow\uparrow}^O(x, x', \omega) &= \frac{\eta uv}{2i(u^2 - v^2)} e^{-\gamma(x+x')} \left[\frac{b_{72} e^{-ik_F(x+x')}}{q_h^S} - \frac{b_{61} e^{ik_F(x+x')}}{q_e^S} \right] \\ &\quad - \frac{\eta}{2i(u^2 - v^2)} e^{-\gamma(x+x')} \frac{a_{62} \cos[k_F(x - x')](k_F + i\gamma(u^2 - v^2))}{(k_F^2 + \gamma^2)} \\ &= -f_{\downarrow\downarrow}^O(x, x', \omega), \quad \text{for } x > 0, \end{aligned} \quad (12)$$

where the normal (b_{61} , b_{72}) and Andreev reflection amplitudes (a_{11} , a_{62}) are calculated from the wavefunctions in Eq. (4) by imposing the boundary conditions Eqs. (6,7) of SM. From Eq. (11) we notice that at $\omega = 0$, Even-EST superconducting pairing depends on $\sin[k_F(x - x')]e^{-\gamma(x+x')}$, showing an oscillatory decay with period $\frac{2\pi}{k_F}$. Even-EST and Odd-EST superconducting pairing as a function of x in superconducting region in presence of spin flip scattering are plotted in Fig. 5. We consider two cases: (a) when zero energy YSR states appear and, (b) when zero energy YSR states are absent. From Fig. 5(a) we notice that for parameters wherein zero energy YSR states occur, Odd-EST pairing is much larger than Even-EST pairing. However, when zero energy YSR states are absent, Even-EST pairing is much larger than Odd-EST pairing as shown in Fig. 5(b). Thus, our results indicate that Odd-EST pairing is enhanced considerably due to the occurrence of zero energy YSR states.

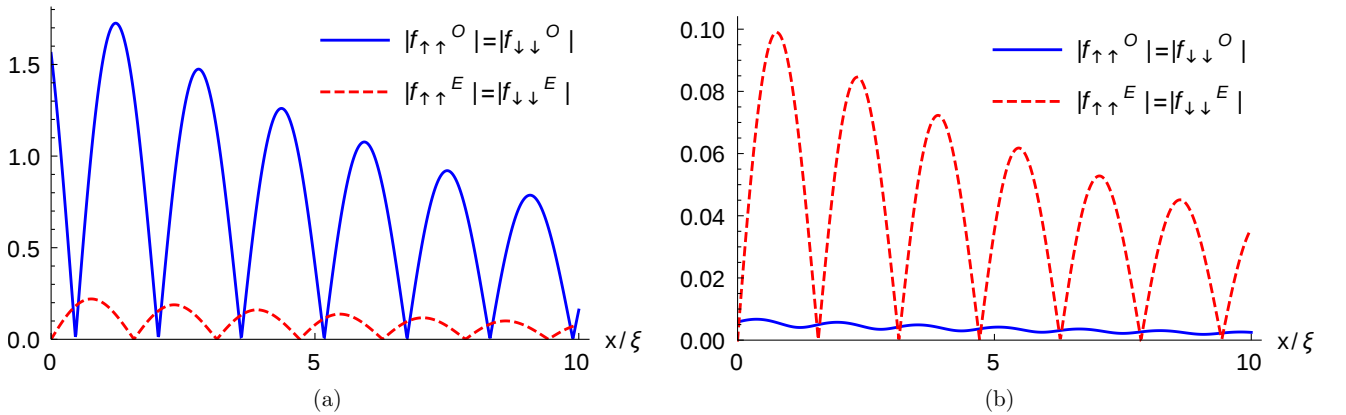


FIG. 5: The magnitudes of the Even-EST and Odd-EST pairing induced vs. position x for (a) when zero energy YSR states occur and for (b) when zero energy YSR states are absent. Parameters: $S = \frac{19}{2}$ (Fig. 5(a)), $S = \frac{9}{2}$ (Fig. 5(b)), $\mathcal{F} = \mathcal{F}' = 10$ (Fig. 5(a)), $\mathcal{F} = \mathcal{F}' = 5$ (Fig. 5(b)), $Z = 0.78$, $\mathcal{J} = 0.4$ (Fig. 5(a)), $\mathcal{J} = 2$ (Fig. 5(b)), $x' = 0$, $k_F a = 0.8437\pi$ (Fig. 5(a)), $k_F a = \pi$ (Fig. 5(b)), $\omega = 0$, $E_F = 10\Delta$.

B. Odd-frequency pairing and YSR bound states in S-N₁-SF-N₂-S Josephson junction

1. Induced spin singlet superconducting pairing in S-N₁-SF-N₂-S Josephson junction

We compute even and odd-frequency SS pairing amplitudes from anomalous components of $G^r(x, x', \omega)$ using Eqs. (6), (7) and (8). For Even-SS and Odd-SS superconducting pairing we get,

$$f_0^E(x, x', \omega) = \frac{\eta uv}{2i(u^2 - v^2)} e^{-\gamma|x-x'|} \left[\frac{e^{ik_F|x-x'|}}{q_e^S} + \frac{e^{-ik_F|x-x'|}}{q_h^S} \right] + \frac{\eta uv}{2i(u^2 - v^2)} e^{\gamma(x+x')} \left[\frac{b'_{11} e^{-ik_F(x+x')}}{q_e^S} + \frac{a'_{42} e^{ik_F(x+x')}}{q_h^S} \right] \\ + \frac{\eta}{2i(u^2 - v^2)} e^{\gamma(x+x')} \cos[k_F(x - x')] \left[\frac{a'_{12} v^2}{q_e^S} + \frac{a'_{41} u^2}{q_h^S} \right], \quad \text{for } x < 0 \quad (13)$$

$$f_0^O(x, x', \omega) = \frac{\eta(a'_{12} v^2 (k_F - i\gamma) - a'_{41} u^2 (k_F + i\gamma))}{2(u^2 - v^2)(k_F^2 + \gamma^2)} e^{\gamma(x+x')} \sin[k_F(x - x')], \quad \text{for } x < 0. \quad (14)$$

From Eq. (13) we notice that Even-SS superconducting pairing depends on both Andreev reflection (a'_{12} , a'_{41} , a'_{42}) and normal reflection amplitudes (b'_{11}), while in Eq. (14) Odd-SS superconducting pairing depends only on Andreev reflection amplitudes (a'_{12} , a'_{41}). The normal and Andreev reflection amplitudes b'_{11} mean normal reflection of incident electron with spin up as electron with spin up, a'_{12} mean Andreev reflection of incident electron with spin up as hole with spin down, similarly a'_{41} and a'_{42} are defined, see supplementary material below Eq. (5) for details. At $x = x'$ local Odd-SS pairing vanishes, while local Even-SS pairing is finite and is maximum.

In Fig. 6, we plot Even-SS and Odd-SS superconducting pairings induced in left superconducting and metallic regions. We consider two cases: (a) when zero energy YSR states occur and (b) when zero energy YSR states are absent. From Fig. 6(a), we see that for $\mathcal{J} = 0.1267$ when zero energy YSR states occur (see Fig. 3(a)), Odd-SS pairing is much larger than Even-SS pairing. However, for $\mathcal{J} = 1$, when zero energy YSR states are absent (see Fig. 3(b)), Even-SS pairing is much more prominent while Odd-SS pairing vanishes as shown in Fig. 6(b). Thus, in the presence of YSR states, there is a vast enhancement of Odd-SS pairing magnitude.

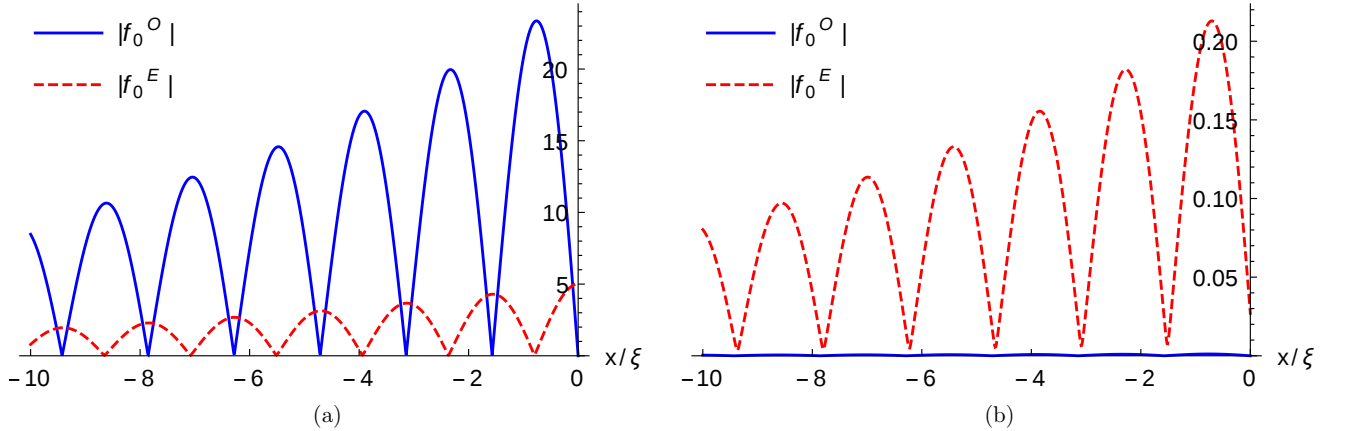


FIG. 6: The magnitudes of the induced Even-SS and Odd-SS pairing vs. position x for (a) when zero energy YSR states occur and for (b) when zero energy YSR states are absent. Parameters: $S = \frac{21}{2}$, $\mathcal{F} = \mathcal{F}' = 11$, $Z = 0.1$, $\mathcal{J} = 0.1267$ (Fig. 6(a)), $\mathcal{J} = 1$ (Fig. 6(b)), $x' = 0$, $E_F = 10\Delta$, $k_F a = \pi$, $\omega = 0$, $\varphi = \pi/2$, $T = 0$.

2. Induced spin triplet superconducting pairing in S-N₁-SF-N₂-S Josephson junction

Next, we compute the induced Even-ST and Odd-ST pairing in S-N₁-SF-N₂-S junction. In this paper, as mentioned in section III.A.2 MST pairing vanishes and only EST pairing is finite as there is absence of spin mixing in our setup, see Ref. [3] for the reasons behind it. Using Eq. (8), the induced Even-EST and Odd-EST superconducting pairings

are,

$$f_{\uparrow\uparrow}^E(x, x', \omega) = \frac{\eta}{2(u^2 - v^2)(k_F^2 + \gamma^2)} e^{\gamma(x+x')} \sin[k_F(x - x')] \left[\frac{a'_{11}v^2}{q_e^S} + \frac{a'_{42}u^2}{q_h^S} \right] = -f_{\downarrow\downarrow}^E(x, x', \omega), \quad \text{for } x < 0 \quad (15)$$

$$\begin{aligned} f_{\uparrow\uparrow}^O(x, x', \omega) = & -\frac{\eta uv}{2i(u^2 - v^2)} e^{\gamma(x+x')} \left[\frac{b'_{12}e^{-ik_F(x+x')}}{q_e^S} + \frac{b'_{41}e^{ik_F(x+x')}}{q_h^S} \right] \\ & - \frac{\eta}{2i(u^2 - v^2)(k_F^2 + \gamma^2)} e^{\gamma(x+x')} \cos[k_F(x - x')] \left[\frac{a'_{11}v^2}{q_e^S} + \frac{a'_{42}u^2}{q_h^S} \right] \\ = & -f_{\downarrow\downarrow}^O(x, x', \omega), \quad \text{for } x < 0. \end{aligned} \quad (16)$$

From Eqs. (15) and, (16) we notice that the induced Even-EST pairing depends only on Andreev reflection amplitudes (a'_{11} , a'_{42}), while the induced Odd-EST pairing depends on both normal (b'_{12} , b'_{41}) as well as Andreev reflection amplitudes (a'_{11} , a'_{42}). At $x = x'$, the induced Even-EST pairing vanishes, while the induced Odd-EST pairing is finite.

In Fig. 7, we plot the induced Even-EST and Odd-EST superconducting pairing in left superconducting and metallic regions vs. position x . Similar to Fig. 6, we consider two cases: (a) when zero energy YSR states occur and (b) when zero energy YSR states are absent. From Fig. 7(a), we notice that for $\mathcal{J} = 0.1267$ when zero energy YSR states occur, the induced Odd-EST pairing dominates over Even-EST pairing. However, for $\mathcal{J} = 1$ when zero energy YSR states are absent, the induced Even-EST pairing is much larger than the Odd-EST pairing, as seen from Fig. 7(b). This suggests a boost to Odd-EST pairing due to zero energy YSR bound states.

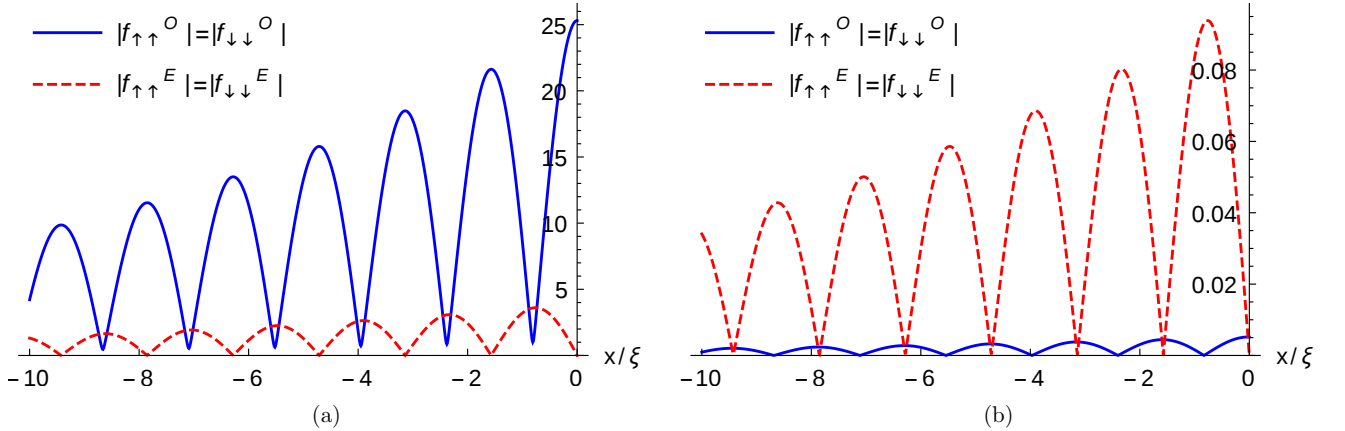


FIG. 7: The magnitudes of the induced Even-EST and Odd-EST superconductor pairing in the left superconducting and normal metal regions vs position x for (a) when zero energy YSR states occur and for (b) when zero energy YSR states are absent. Parameters: $S = \frac{21}{2}$, $\mathcal{F} = \mathcal{F}' = 11$, $Z = 0.1$, $\mathcal{J} = 0.1267$ (Fig. 7(a)), $\mathcal{J} = 1$ (Fig. 7(b)), $x' = 0$, $E_F = 10\Delta$, $k_F a = \pi$, $\omega = 0$, $\varphi = \pi/2$, $T = 0$.

IV. ANALYSIS

In this section, we analyze our results. Table I compares our results when zero energy YSR states occur and when they are absent in N-sf-N-S and S-N-sf-N-S junctions. For zero energy YSR states, we see an almost quantized (at $2e^2/h$) zero-bias peak in the conductance spectra, while no such zero-bias conductance peaks are present when zero energy YSR states are absent. The signatures of YSR states are also detected via the induced odd and even frequency pairing. We find that induced odd-frequency superconducting pairing is enhanced multi-fold over even frequency pairing due to the presence of YSR states. For S-N-sf-N-S Josephson junction, $0 - \pi$ junction transition occurs in the presence of zero energy YSR states, and induced odd-frequency superconducting pairing is much larger than even frequency superconducting pairing. However, in the absence of zero energy YSR states that no $0 - \pi$ junction transition occurs, and induced even frequency superconducting pairing is much more prominent while odd-frequency

pairing vanishes. A multifold enhancement of the induced odd-frequency pairing is a signature of YSR bound states for both N-sf-N-S and S-N-sf-N-S junctions.

TABLE I: Comparing induced odd ω pairing in presence and absence of zero energy YSR states

	Zero energy YSR states occur	Zero energy YSR states are absent
N-sf-N-S	(1) Almost quantized zero bias conductance peak.	(1) No zero bias conductance peak.
	(2) Induced odd-frequency pairing (both singlet and equal spin triplet) dominates even frequency pairing.	(2) Induced even frequency pairing (both singlet and equal spin triplet) dominates odd-frequency pairing.
S-N-sf-N-S	(1) There is a $0 - \pi$ junction transition when zero energy YSR states occur.	(1) There is no $0 - \pi$ junction transition.
	(2) Odd-frequency superconducting pairing is enhanced multi-fold over even frequency superconducting pairing	(2) Even frequency superconducting pairing is much larger with vanishing odd-frequency superconducting pairing.

V. EXPERIMENTAL REALIZATION AND CONCLUSION

As shown in Fig. 1, our setups can be experimentally realized easily since the metal-superconductor junctions were realized in a lab around 45 years ago[31]. Placing a spin flipper at the metal-superconductor interface should not be cumbersome; particularly with a conventional superconductor, it should be possible.

In this work, we see a strong correlation between odd-frequency superconductivity and the occurrence of zero energy YSR states in both metal-spin flipper-metal-s-wave superconductor junction as well as in superconductor-metal-spin flipper-metal-superconductor junction. For metal-spin flipper-metal-s-wave superconductor junction, we notice that in a parameter regime wherein zero energy YSR states occur, the induced odd-frequency pairing is much larger than even frequency pairing. But, for parameters for which zero energy YSR states are absent, the opposite occurs, i.e., even frequency pairing is much larger than odd-frequency pairing. In the case of superconductor-metal-spin flipper-metal-superconductor junction, when zero energy YSR states occur, $0 - \pi$ junction transition is seen, and odd-frequency pairing dominates even frequency pairing. Our findings imply that the occurrence of large odd-frequency pairing can be a fingerprint for YSR states.

-
- [1] M. Sigrist and K. Ueda, Phenomenological theory of unconventional superconductivity, *Rev. Mod. Phys.* 63, 239 (1991).
 - [2] V. L. Berezinskii, New model of the anisotropic phase of superfluid ^3He , *Zh. Eksp. Teor. Fiz.* 20, 628 (1974) [*JETP Lett.* 20, 287 (1974)].
 - [3] S. Pal and C. Benjamin, Exciting odd-frequency equal spin-triplet correlations at metal-superconductor interfaces, *Phys. Rev. B* 104, 054519 (2021).
 - [4] L. Yu, Bound state in superconductors with paramagnetic impurities, *Acta Phys. Sin.* 21, 75 (1965).
 - [5] H. Shiba, Classical Spins in Superconductors, *Prog. Theor. Phys.* 40, 435 (1968).
 - [6] A. I. Rusinov, superconductivity near a paramagnetic impurity, *Zh. Eksp. Teor. Fiz. Pisma Red.* 9, 146 (1968).
 - [7] S. Pal and C. Benjamin, Yu-Shiba-Rusinov bound states induced by a spin flipper in the vicinity of an s-wave superconductor, *Sci. Rep.* 8, 11949 (2018).
 - [8] D. Persson et al., Spin-polarized currents and noise in normal-metal/superconductor junctions with Yu-Shiba-Rusinov impurities, *Phys. Rev. B* 94, 155424 (2016).
 - [9] A. Costa, J. Fabian, and D. Kochan, Connection between zero-energy Yu-Shiba-Rusinov states and $0-\pi$ transitions in magnetic Josephson junctions, *Phys. Rev. B* 98, 134511 (2018).
 - [10] A. Yazdani et al., Probing the Local Effects of Magnetic Impurities on Superconductivity, *Science* 275, 1767 (1997).
 - [11] K. J. Franke, G. Schulze, & J. I. Pascual, Competition of Superconducting Phenomena and Kondo Screening at the Nanoscale, *Science* 332, 940 (2011).
 - [12] M. Ruby et al., Tunneling Processes into Localized Subgap States in Superconductors, *Phys. Rev. Lett.* 115, 087001 (2015).
 - [13] S-I. Suzuki, T. Sato, and Y. Asano, An odd-frequency Cooper pair around a magnetic impurity, *arXiv:2204.03242*.
 - [14] M. Eschrig, Spin-polarized supercurrents for spintronics: a review of current progress, *Rep. Prog. Phys.* 78, 104501 (2015).
 - [15] J. Linder and J. W. A Robinson, Superconducting spintronics, *Nat. Phys.* 11, 307-315 (2015).
 - [16] R. Pawlak et al., Probing atomic structure and Majorana wavefunctions in mono-atomic Fe chains on superconducting Pb surface, *npj Quantum Information* 2, 16035 (2016).

- [17] See supplementary material for wavefunctions and boundary conditions of our model and the details procedure on how we compute retarded Green's functions.
- [18] G. E. Blonder, M. Tinkham and T. M. Klapwijk, Transition from metallic to tunneling regimes in superconducting microconstrictions: Excess current, charge imbalance, and supercurrent conversion, Phys. Rev. B 25, 4515 (1982).
- [19] O. L. T de Menezes and J.S Helman, Spin flip enhancement at resonant transmission, Am. J. Phys 53, 1100 (1985).
- [20] H. D. Liu, X. X. Yi, Geometric phases in a scattering process, Phys. Rev. A 84, 022114 (2011).
- [21] G. Coudourier-Maruri, Y. Omar, R. de Coss, and S. Bose, Graphene-enabled low-control quantum gates between static and mobile spins, Phys. Rev. B 89, 075426 (2014).
- [22] F. Ciccarello, G. M. Palma, and M. Zarcione, Entanglement-induced electron coherence in a mesoscopic ring with two magnetic impurities, Phys. Rev. B 75, 205415 (2007).
- [23] Q. Cheng, B. Jin, Quantum transport in normal-metal/ferromagnet/spin-triplet superconductor junctions, Physica B 426, 42 (2013).
- [24] S. Kashiwaya et al., Spin current in ferromagnet-insulator-superconductor junctions, Phys. Rev. B 60, 3572 (1999).
- [25] A. A. Golubov, M. Y. Kupriyanov, & E. Il'ichev, The current-phase relation in Josephson junctions, Rev. Mod. Phys. 76, 411 (2004).
- [26] W. L. McMillan, Theory of Superconductor-Normal-Metal Interfaces, Phys. Rev. 175, 559 (1968).
- [27] J. Cayao and A. M. Black-Schaffer, Odd-frequency superconducting pairing and subgap density of states at the edge of a two-dimensional topological insulator without magnetism, Phys. Rev. B 96, 155426 (2017).
- [28] J. Cayao and A. M. Black-Schaffer, Odd-frequency superconducting pairing in junctions with Rashba spin-orbit coupling, Phys. Rev. B 98, 075425 (2018).
- [29] H. Enoksen, J. Linder, & A. Sudbø, Spin-flip scattering and critical currents in ballistic half-metallic *d*-wave Josephson junctions, Phys. Rev. B 85, 014512 (2012).
- [30] G. Annunziata, H. Enoksen, J. Linder, M. cuoco, C. Noce and A. Sudbo, Josephson effect in S/F/S junctions: Spin bandwidth asymmetry versus Stoner exchange, Phys. Rev. B 83, 144520 (2011).
- [31] G. Gusman, J. F. Thomas, R. Deltour, Normal-metal-insulator-superconductor tunnel-junction study of the magnetic field dependence of superconducting thin films, Phys. Rev. B 16, 3165 (1977).

Appendix A: Supplementary Material for “Yu-Shiba-Rusinov bound states boost odd-frequency superconductivity”, by Subhajit Pal and Colin Benjamin

In this supplementary material, we first provide wavefunctions and boundary conditions for our two setups to calculate Yu-Shiba-Rusinov bound states, Josephson current, and Green's functions. After that, we discuss the procedure to calculate energy-bound shapes and retarded Green's functions for our setup. Finally, we also give an explicit form of expressions for anomalous Green's functions.

1. Wavefunctions and boundary conditions in the metal-spin flipper-metal-superconductor junction and superconductor-metal-spin flipper-metal-superconductor junction

We choose two setups first, 1D metal (N)-metal (N)-*s*-wave superconductor (S) junction with a spin-flipper (sf) between the two metals as depicted in Fig. 1(a), and second, two metals with an embedded spin-flipper between two *s*-wave superconductors as shown in Fig. 1(b). The Hamiltonian for spin-flipper is mentioned in Eq. (1). The model Hamiltonian in BdG formalism for metal-spin-flipper-metal-superconductor (N_1 -sf- N_2 -S) junction as shown in Fig. 1(a) is given in Eq. (2), while the model Hamiltonian in BdG formalism for superconductor-metal-spin-flipper-metal-superconductor (S- N_1 -sf- N_2 -S) junction as shown in Fig. 1(b) is given in Eq. (3).

a. Wavefunctions in metal-spin flipper-metal-superconductor junction

After diagonalizing the Hamiltonian (2), the wavefunctions in different domains of metal-spin flipper-metal-superconductor junction for various kinds of scattering processes are obtained. The wavefunctions are-

$$\begin{aligned}
 \varphi_1(x) &= \begin{cases} \chi_1^N e^{iq_e(x+a)} \phi_{m'}^S + a_{11} \chi_3^N e^{iq_h(x+a)} \phi_{m'+1}^S + a_{12} \chi_4^N e^{iq_h(x+a)} \phi_{m'}^S + b_{11} \chi_1^N e^{-iq_e(x+a)} \phi_{m'}^S + b_{12} \chi_2^N e^{-iq_e(x+a)} \phi_{m'+1}^S, & x < -a \\ c_{11} \chi_1^N e^{iq_e(x+a)} \phi_{m'}^S + c_{12} \chi_2^N e^{iq_e(x+a)} \phi_{m'+1}^S + d_{11} \chi_1^N e^{-iq_e x} \phi_{m'}^S + d_{12} \chi_2^N e^{-iq_e x} \phi_{m'+1}^S + e_{11} \chi_3^N e^{iq_h x} \phi_{m'+1}^S + e_{12} \chi_4^N e^{iq_h x} \phi_{m'}^S, & -a < x < 0 \\ g_{11} \chi_1^S e^{iq_e^S x} \phi_{m'}^S + g_{12} \chi_2^S e^{iq_e^S x} \phi_{m'+1}^S + h_{11} \chi_3^S e^{-iq_h^S x} \phi_{m'+1}^S + h_{12} \chi_4^S e^{-iq_h^S x} \phi_{m'}^S, & x > 0 \end{cases} \\
 \varphi_2(x) &= \begin{cases} \chi_2^N e^{iq_e(x+a)} \phi_{m'}^S + a_{21} \chi_3^N e^{iq_h(x+a)} \phi_{m'}^S + a_{22} \chi_4^N e^{iq_h(x+a)} \phi_{m'-1}^S + b_{21} \chi_1^N e^{-iq_e(x+a)} \phi_{m'-1}^S + b_{22} \chi_2^N e^{-iq_e(x+a)} \phi_{m'}^S, & x < -a \\ c_{21} \chi_1^N e^{iq_e(x+a)} \phi_{m'-1}^S + c_{22} \chi_2^N e^{iq_e(x+a)} \phi_{m'}^S + d_{21} \chi_1^N e^{-iq_e x} \phi_{m'-1}^S + d_{22} \chi_2^N e^{-iq_e x} \phi_{m'}^S + e_{21} \chi_3^N e^{iq_h x} \phi_{m'}^S + e_{22} \chi_4^N e^{iq_h x} \phi_{m'-1}^S, & -a < x < 0 \\ g_{21} \chi_1^S e^{iq_e^S x} \phi_{m'-1}^S + g_{22} \chi_2^S e^{iq_e^S x} \phi_{m'}^S + h_{21} \chi_3^S e^{-iq_h^S x} \phi_{m'}^S + h_{22} \chi_4^S e^{-iq_h^S x} \phi_{m'-1}^S, & x > 0 \end{cases} \\
 \varphi_3(x) &= \begin{cases} \chi_3^N e^{-iq_h(x+a)} \phi_{m'}^S + a_{31} \chi_1^N e^{iq_e(x+a)} \phi_{m'-1}^S + a_{32} \chi_2^N e^{iq_e(x+a)} \phi_{m'}^S + b_{31} \chi_3^N e^{-iq_h(x+a)} \phi_{m'}^S + b_{32} \chi_4^N e^{-iq_h(x+a)} \phi_{m'-1}^S, & x < -a \\ c_{31} \chi_1^N e^{iq_e(x+a)} \phi_{m'-1}^S + c_{32} \chi_2^N e^{iq_e(x+a)} \phi_{m'}^S + d_{31} \chi_1^N e^{-iq_e x} \phi_{m'-1}^S + d_{32} \chi_2^N e^{-iq_e x} \phi_{m'}^S + e_{31} \chi_3^N e^{iq_h x} \phi_{m'}^S + e_{32} \chi_4^N e^{iq_h x} \phi_{m'-1}^S, & -a < x < 0 \\ g_{31} \chi_1^S e^{iq_e^S x} \phi_{m'-1}^S + g_{32} \chi_2^S e^{iq_e^S x} \phi_{m'}^S + h_{31} \chi_3^S e^{-iq_h^S x} \phi_{m'}^S + h_{32} \chi_4^S e^{-iq_h^S x} \phi_{m'-1}^S, & x > 0 \end{cases} \\
 \varphi_4(x) &= \begin{cases} \chi_4^N e^{-iq_h(x+a)} \phi_{m'}^S + a_{41} \chi_1^N e^{iq_e(x+a)} \phi_{m'}^S + a_{42} \chi_2^N e^{iq_e(x+a)} \phi_{m'+1}^S + b_{41} \chi_3^N e^{-iq_h(x+a)} \phi_{m'+1}^S + b_{42} \chi_4^N e^{-iq_h(x+a)} \phi_{m'}^S, & x < -a \\ c_{41} \chi_1^N e^{iq_e(x+a)} \phi_{m'}^S + c_{42} \chi_2^N e^{iq_e(x+a)} \phi_{m'+1}^S + d_{41} \chi_1^N e^{-iq_e x} \phi_{m'}^S + d_{42} \chi_2^N e^{-iq_e x} \phi_{m'+1}^S + e_{41} \chi_3^N e^{iq_h x} \phi_{m'+1}^S + e_{42} \chi_4^N e^{iq_h x} \phi_{m'}^S, & -a < x < 0 \\ g_{41} \chi_1^S e^{iq_e^S x} \phi_{m'}^S + g_{42} \chi_2^S e^{iq_e^S x} \phi_{m'+1}^S + h_{41} \chi_3^S e^{-iq_h^S x} \phi_{m'+1}^S + h_{42} \chi_4^S e^{-iq_h^S x} \phi_{m'}^S, & x > 0 \end{cases} \\
 \varphi_5(x) &= \begin{cases} g_{51} \chi_1^N e^{iq_e(x+a)} \phi_{m'}^S + g_{52} \chi_2^N e^{iq_e(x+a)} \phi_{m'+1}^S + h_{51} \chi_3^N e^{-iq_h(x+a)} \phi_{m'+1}^S + h_{52} \chi_4^N e^{-iq_h(x+a)} \phi_{m'}^S, & x < -a \\ c_{51} \chi_1^N e^{iq_e(x+a)} \phi_{m'}^S + c_{52} \chi_2^N e^{iq_e(x+a)} \phi_{m'+1}^S + d_{51} \chi_1^N e^{-iq_e x} \phi_{m'}^S + d_{52} \chi_2^N e^{-iq_e x} \phi_{m'+1}^S + e_{51} \chi_3^N e^{iq_h x} \phi_{m'+1}^S + e_{52} \chi_4^N e^{iq_h x} \phi_{m'}^S, & -a < x < 0 \\ \chi_1^S e^{-iq_e^S x} \phi_{m'}^S + a_{51} \chi_2^S e^{-iq_e^S x} \phi_{m'+1}^S + a_{52} \chi_3^S e^{-iq_h^S x} \phi_{m'}^S + b_{51} \chi_1^S e^{iq_e^S x} \phi_{m'}^S + b_{52} \chi_2^S e^{iq_e^S x} \phi_{m'+1}^S, & x > 0 \end{cases} \\
 \varphi_6(x) &= \begin{cases} g_{61} \chi_1^N e^{iq_e(x+a)} \phi_{m'-1}^S + g_{62} \chi_2^N e^{iq_e(x+a)} \phi_{m'}^S + h_{61} \chi_3^N e^{-iq_h(x+a)} \phi_{m'}^S + h_{62} \chi_4^N e^{-iq_h(x+a)} \phi_{m'-1}^S, & x < -a \\ c_{61} \chi_1^N e^{iq_e(x+a)} \phi_{m'-1}^S + c_{62} \chi_2^N e^{iq_e(x+a)} \phi_{m'}^S + d_{61} \chi_1^N e^{-iq_e x} \phi_{m'-1}^S + d_{62} \chi_2^N e^{-iq_e x} \phi_{m'}^S + e_{61} \chi_3^N e^{iq_h x} \phi_{m'}^S + e_{62} \chi_4^N e^{iq_h x} \phi_{m'-1}^S, & -a < x < 0 \\ \chi_2^S e^{-iq_e^S x} \phi_{m'}^S + a_{61} \chi_3^S e^{-iq_h^S x} \phi_{m'}^S + a_{62} \chi_4^S e^{-iq_h^S x} \phi_{m'-1}^S + b_{61} \chi_1^S e^{iq_e^S x} \phi_{m'-1}^S + b_{62} \chi_2^S e^{iq_e^S x} \phi_{m'}^S, & x > 0 \end{cases} \\
 \varphi_7(x) &= \begin{cases} g_{71} \chi_1^N e^{iq_e(x+a)} \phi_{m'-1}^S + g_{72} \chi_2^N e^{iq_e(x+a)} \phi_{m'}^S + h_{71} \chi_3^N e^{-iq_h(x+a)} \phi_{m'}^S + h_{72} \chi_4^N e^{-iq_h(x+a)} \phi_{m'-1}^S, & x < -a \\ c_{71} \chi_1^N e^{iq_e(x+a)} \phi_{m'-1}^S + c_{72} \chi_2^N e^{iq_e(x+a)} \phi_{m'}^S + d_{71} \chi_1^N e^{-iq_e x} \phi_{m'-1}^S + d_{72} \chi_2^N e^{-iq_e x} \phi_{m'}^S + e_{71} \chi_3^N e^{iq_h x} \phi_{m'}^S + e_{72} \chi_4^N e^{iq_h x} \phi_{m'-1}^S, & -a < x < 0 \\ \chi_3^S e^{iq_h^S x} \phi_{m'}^S + a_{71} \chi_1^S e^{-iq_e^S x} \phi_{m'-1}^S + a_{72} \chi_2^S e^{-iq_e^S x} \phi_{m'}^S + b_{71} \chi_3^S e^{iq_h^S x} \phi_{m'}^S + b_{72} \chi_4^S e^{iq_h^S x} \phi_{m'-1}^S, & x > 0 \end{cases} \\
 \varphi_8(x) &= \begin{cases} g_{81} \chi_1^N e^{iq_e(x+a)} \phi_{m'}^S + g_{82} \chi_2^N e^{iq_e(x+a)} \phi_{m'+1}^S + h_{81} \chi_3^N e^{-iq_h(x+a)} \phi_{m'+1}^S + h_{82} \chi_4^N e^{-iq_h(x+a)} \phi_{m'}^S, & x < -a \\ c_{81} \chi_1^N e^{iq_e(x+a)} \phi_{m'}^S + c_{82} \chi_2^N e^{iq_e(x+a)} \phi_{m'+1}^S + d_{81} \chi_1^N e^{-iq_e x} \phi_{m'}^S + d_{82} \chi_2^N e^{-iq_e x} \phi_{m'+1}^S + e_{81} \chi_3^N e^{iq_h x} \phi_{m'+1}^S + e_{82} \chi_4^N e^{iq_h x} \phi_{m'}^S, & -a < x < 0 \\ \chi_4^S e^{iq_h^S x} \phi_{m'}^S + a_{81} \chi_1^S e^{-iq_e^S x} \phi_{m'}^S + a_{82} \chi_2^S e^{-iq_e^S x} \phi_{m'+1}^S + b_{81} \chi_3^S e^{iq_h^S x} \phi_{m'+1}^S + b_{82} \chi_4^S e^{iq_h^S x} \phi_{m'}^S, & x > 0 \end{cases}
 \end{aligned} \tag{A1}$$

where $\chi_1^N = \begin{bmatrix} 1 \\ 0 \\ 0 \\ 0 \end{bmatrix}$, $\chi_2^N = \begin{bmatrix} 0 \\ 1 \\ 0 \\ 0 \end{bmatrix}$, $\chi_3^N = \begin{bmatrix} 0 \\ 0 \\ 1 \\ 0 \end{bmatrix}$, $\chi_4^N = \begin{bmatrix} 0 \\ 0 \\ 0 \\ 1 \end{bmatrix}$, $\chi_1^S = \begin{bmatrix} u \\ 0 \\ 0 \\ v \end{bmatrix}$, $\chi_2^S = \begin{bmatrix} 0 \\ -u \\ v \\ 0 \end{bmatrix}$, $\chi_3^S = \begin{bmatrix} 0 \\ -v \\ u \\ 0 \end{bmatrix}$ and $\chi_4^S = \begin{bmatrix} v \\ 0 \\ 0 \\ u \end{bmatrix}$. In

Eq. (A1), φ_1 , φ_2 , φ_3 , and φ_4 represent the wavefunctions when spin up electron, spin down electron, spin up hole and spin down hole are injected from left metallic region respectively, while φ_5 , φ_6 , φ_7 , and φ_8 represent the wavefunctions when spin up electronlike quasiparticle, spin down electronlike quasiparticle, spin up holelike quasiparticle and spin down holelike quasiparticle are injected from superconductor respectively. a_{ij} and b_{ij} represent Andreev and normal reflection coefficient respectively, while g_{ij} and h_{ij} represent transmission coefficients for electron/electronlike and hole/holelike quasiparticles respectively with $i = 1, 2, \dots, 8$ and $j = 1, 2$, where $i = 1$ means electron up incident from left, $i = 2$ means electron down incident from left, $i = 3$ means hole up incident from left, $i = 4$ means hole down incident from left, $i = 5$ means spin up electronlike quasiparticle incident from right, $i = 6$ means spin down electronlike quasiparticle incident from right, $i = 7$ means spin up holelike quasiparticle incident from right and, finally $i = 8$ means spin down holelike quasiparticle incident from right. In a_{ij} , $j = 1$ means hole up reflected back to left and, $j = 2$ means hole down reflected back to left when $i = 1, 2$, while $j = 1$ means electron up reflected back to left and, $j = 2$ means electron down reflected back to left when $i = 3, 4$. Similarly, when $i = 5, 6$, $j = 1$ means holelike quasiparticle with spin up reflected back to right and, $j = 2$ means holelike quasiparticle with spin down reflected back to right, while $j = 1$ means electronlike quasiparticle with spin up reflected back to right and, $j = 2$ means electronlike quasiparticle with spin down reflected back to right when $i = 7, 8$. In b_{ij} , $j = 1$ means electron up reflected back to left and, $j = 2$ means electron down reflected back to left for $i = 1, 2$, while for $i = 3, 4$, $j = 1$ means hole up reflected back to left and, $j = 2$ means hole down reflected back to left. Further, in b_{ij} , $j = 1$ means

electronlike quasiparticle with spin up reflected back to right and, $j = 2$ means electronlike quasiparticle with spin down reflected back to right when $i = 5, 6$, while for $i = 7, 8$, $j = 1$ means holelike quasiparticle with spin up reflected back to right and, $j = 2$ means holelike quasiparticle with spin down reflected back to right. In g_{ij} , $j = 1$ means spin up electronlike quasiparticle transmitted into right and, $j = 2$ means spin down electronlike quasiparticle transmitted into right for $i = 1, 2, 3, 4$, while $j = 1$ means spin up electron transmitted into left and, $j = 2$ means spin down electron transmitted into left for $i = 5, 6, 7, 8$. Finally, in h_{ij} , $j = 1$ means spin up holelike quasiparticle transmitted into right and, $j = 2$ means spin down holelike quasiparticle transmitted into right for $i = 1, 2, 3, 4$, while $j = 1$ means spin up hole transmitted into left and, $j = 2$ means spin down hole transmitted into left for $i = 5, 6, 7, 8$. The spin flipper's eigenfunction is represented by $\phi_{m'}^S$ with its spin S and spin magnetic moment m' . The z component of spin flipper's spin S^z is acting as- $S^z \phi_{m'}^S = \hbar m' \phi_{m'}^S$. $u = \sqrt{\frac{1}{2}(\frac{\omega + \sqrt{\omega^2 - \Delta^2}}{\omega})}$ and $v = \sqrt{\frac{1}{2}(\frac{\omega - \sqrt{\omega^2 - \Delta^2}}{\omega})}$ are the BCS coherence factors. $q_{e,h} = \sqrt{\frac{2m^*}{\hbar^2}(E_F \pm \omega)}$ is the wave-vector in normal metal, while $q_{e,h}^S = \sqrt{\frac{2m^*}{\hbar^2}(E_F \pm \sqrt{\omega^2 - \Delta^2})}$ is the wave-vector in superconductor. If we diagonalize the Hamiltonian $H_{BdG}^*(-k)$ instead of $H_{BdG}(k)$ we will get conjugated processes $\tilde{\psi}_i$ which is necessary to form the retarded Green's functions in next section. For our setup (Fig. 1) we note that $\tilde{\chi}_i^{N(S)} = \chi_i^{N(S)}$. In our work we consider $E_F \gg \Delta, \omega$, in this limit $q_{e,h} \approx k_F(1 \pm \frac{\omega}{2E_F})$ and $q_{e,h}^S \approx k_F \pm i\gamma$ where $k_F = \sqrt{\frac{2m^*E_F}{\hbar^2}}$ and $\gamma = \sqrt{\Delta^2 - \omega^2}[k_F/(2E_F)]$. $\xi = \frac{\hbar}{m^*\Delta}$ is the superconducting coherence length.

2. Wavefunctions in superconductor-metal-spin flipper-metal-superconductor junction

After diagonalizing the Hamiltonian (3), the wavefunctions in different domains of superconductor-metal-spin flipper-metal-superconductor junction for various kinds of scattering processes are obtained. The wavefunctions are-

$$\begin{aligned}
 \varphi_1(x) &= \begin{cases} \chi_1^S e^{iq_e^S x} \phi_{m'}^S + a'_{11} \chi_3^S e^{iq_h^S x} \phi_{m'+1}^S + a'_{12} \chi_4^S e^{iq_h^S x} \phi_{m'}^S + b'_{11} \chi_1^S e^{-iq_e^S x} \phi_{m'}^S + b'_{12} \chi_2^S e^{-iq_e^S x} \phi_{m'+1}^S, & x < -a/2, \\ c'_{11} \chi_1^N e^{iq_e(x+a/2)} \phi_{m'}^S + c'_{12} \chi_2^N e^{iq_e(x+a/2)} \phi_{m'+1}^S + d'_{11} \chi_1^N e^{-iq_e x} \phi_{m'}^S + d'_{12} \chi_2^N e^{-iq_e x} \phi_{m'+1}^S + e'_{11} \chi_3^N e^{iq_h x} \phi_{m'+1}^S + e'_{12} \chi_4^N e^{iq_h x} \phi_{m'}^S, & -a/2 < x < 0, \\ f'_{11} \chi_3^N e^{-iq_h(x+a/2)} \phi_{m'+1}^S + f'_{12} \chi_4^N e^{-iq_h(x+a/2)} \phi_{m'}^S, & \\ g'_{11} \chi_1^N e^{-iq_e(x-a/2)} \phi_{m'}^S + g'_{12} \chi_2^N e^{-iq_e(x-a/2)} \phi_{m'+1}^S + h'_{11} \chi_1^N e^{iq_e x} \phi_{m'}^S + h'_{12} \chi_2^N e^{iq_e x} \phi_{m'+1}^S + i'_{11} \chi_3^N e^{-iq_h x} \phi_{m'+1}^S + i'_{12} \chi_4^N e^{-iq_h x} \phi_{m'}^S, & 0 < x < a/2, \\ j'_{11} \chi_3^N e^{iq_h(x-a/2)} \phi_{m'+1}^S + j'_{12} \chi_4^N e^{iq_h(x-a/2)} \phi_{m'}^S, & \\ k'_{11} \chi_1^S e^{iq_e^S x} \phi_{m'}^S + k'_{12} \chi_2^S e^{iq_e^S x} \phi_{m'+1}^S + l'_{11} \chi_3^S e^{-iq_h^S x} \phi_{m'+1}^S + l'_{12} \chi_4^S e^{-iq_h^S x} \phi_{m'}^S, & x > a/2. \end{cases} \\
 \varphi_2(x) &= \begin{cases} \chi_2^S e^{iq_e^S x} \phi_{m'}^S + a'_{21} \chi_3^S e^{iq_h^S x} \phi_{m'}^S + a'_{22} \chi_4^S e^{iq_h^S x} \phi_{m'-1}^S + b'_{21} \chi_1^S e^{-iq_e^S x} \phi_{m'-1}^S + b'_{22} \chi_2^S e^{-iq_e^S x} \phi_{m'}^S, & x < -a/2, \\ c'_{21} \chi_1^N e^{iq_e(x+a/2)} \phi_{m'-1}^S + c'_{22} \chi_2^N e^{iq_e(x+a/2)} \phi_{m'}^S + d'_{21} \chi_1^N e^{-iq_e x} \phi_{m'-1}^S + d'_{22} \chi_2^N e^{-iq_e x} \phi_{m'}^S + e'_{21} \chi_3^N e^{iq_h x} \phi_{m'}^S + e'_{22} \chi_4^N e^{iq_h x} \phi_{m'-1}^S, & -a/2 < x < 0, \\ f'_{21} \chi_3^N e^{-iq_h(x+a/2)} \phi_{m'}^S + f'_{22} \chi_4^N e^{-iq_h(x+a/2)} \phi_{m'-1}^S, & \\ g'_{21} \chi_1^N e^{-iq_e(x-a/2)} \phi_{m'-1}^S + g'_{22} \chi_2^N e^{-iq_e(x-a/2)} \phi_{m'}^S + h'_{21} \chi_1^N e^{iq_e x} \phi_{m'-1}^S + h'_{22} \chi_2^N e^{iq_e x} \phi_{m'}^S + i'_{21} \chi_3^N e^{-iq_h x} \phi_{m'}^S + i'_{22} \chi_4^N e^{-iq_h x} \phi_{m'-1}^S, & 0 < x < a/2, \\ j'_{21} \chi_3^N e^{iq_h(x-a/2)} \phi_{m'}^S + j'_{22} \chi_4^N e^{iq_h(x-a/2)} \phi_{m'-1}^S, & \\ k'_{21} \chi_1^S e^{iq_e^S x} \phi_{m'-1}^S + k'_{22} \chi_2^S e^{iq_e^S x} \phi_{m'}^S + l'_{21} \chi_3^S e^{-iq_h^S x} \phi_{m'}^S + l'_{22} \chi_4^S e^{-iq_h^S x} \phi_{m'-1}^S, & x > a/2. \end{cases} \\
 \varphi_3(x) &= \begin{cases} \chi_3^S e^{-iq_h^S x} \phi_{m'}^S + b'_{31} \chi_3^S e^{iq_h^S x} \phi_{m'}^S + b'_{32} \chi_4^S e^{iq_h^S x} \phi_{m'-1}^S + a'_{31} \chi_1^S e^{-iq_e^S x} \phi_{m'-1}^S + a'_{32} \chi_2^S e^{-iq_e^S x} \phi_{m'}^S, & x < -a/2, \\ c'_{31} \chi_1^N e^{iq_e(x+a/2)} \phi_{m'-1}^S + c'_{32} \chi_2^N e^{iq_e(x+a/2)} \phi_{m'}^S + d'_{31} \chi_1^N e^{-iq_e x} \phi_{m'-1}^S + d'_{32} \chi_2^N e^{-iq_e x} \phi_{m'}^S + e'_{31} \chi_3^N e^{iq_h x} \phi_{m'}^S + e'_{32} \chi_4^N e^{iq_h x} \phi_{m'-1}^S, & -a/2 < x < 0, \\ f'_{31} \chi_3^N e^{-iq_h(x+a/2)} \phi_{m'}^S + f'_{32} \chi_4^N e^{-iq_h(x+a/2)} \phi_{m'-1}^S, & \\ g'_{31} \chi_1^N e^{-iq_e(x-a/2)} \phi_{m'-1}^S + g'_{32} \chi_2^N e^{-iq_e(x-a/2)} \phi_{m'}^S + h'_{31} \chi_1^N e^{iq_e x} \phi_{m'-1}^S + h'_{32} \chi_2^N e^{iq_e x} \phi_{m'}^S + i'_{31} \chi_3^N e^{-iq_h x} \phi_{m'}^S + i'_{32} \chi_4^N e^{-iq_h x} \phi_{m'-1}^S, & 0 < x < a/2, \\ j'_{31} \chi_3^N e^{iq_h(x-a/2)} \phi_{m'}^S + j'_{32} \chi_4^N e^{iq_h(x-a/2)} \phi_{m'-1}^S, & \\ k'_{31} \chi_1^S e^{iq_e^S x} \phi_{m'-1}^S + k'_{32} \chi_2^S e^{iq_e^S x} \phi_{m'}^S + l'_{31} \chi_3^S e^{-iq_h^S x} \phi_{m'}^S + l'_{32} \chi_4^S e^{-iq_h^S x} \phi_{m'-1}^S, & x > a/2. \end{cases} \\
 \varphi_4(x) &= \begin{cases} \chi_4^S e^{-iq_h^S x} \phi_{m'}^S + b'_{41} \chi_3^S e^{iq_h^S x} \phi_{m'+1}^S + b'_{42} \chi_4^S e^{iq_h^S x} \phi_{m'}^S + a'_{41} \chi_1^S e^{-iq_e^S x} \phi_{m'}^S + a'_{42} \chi_2^S e^{-iq_e^S x} \phi_{m'+1}^S, & x < -a/2, \\ c'_{41} \chi_1^N e^{iq_e(x+a/2)} \phi_{m'}^S + c'_{42} \chi_2^N e^{iq_e(x+a/2)} \phi_{m'+1}^S + d'_{41} \chi_1^N e^{-iq_e x} \phi_{m'}^S + d'_{42} \chi_2^N e^{-iq_e x} \phi_{m'+1}^S + e'_{41} \chi_3^N e^{iq_h x} \phi_{m'+1}^S + e'_{42} \chi_4^N e^{iq_h x} \phi_{m'}^S, & -a/2 < x < 0, \\ f'_{41} \chi_3^N e^{-iq_h(x+a/2)} \phi_{m'+1}^S + f'_{42} \chi_4^N e^{-iq_h(x+a/2)} \phi_{m'}^S, & \\ g'_{41} \chi_1^N e^{-iq_e(x-a/2)} \phi_{m'}^S + g'_{42} \chi_2^N e^{-iq_e(x-a/2)} \phi_{m'+1}^S + h'_{41} \chi_1^N e^{iq_e x} \phi_{m'}^S + h'_{42} \chi_2^N e^{iq_e x} \phi_{m'+1}^S + i'_{41} \chi_3^N e^{-iq_h x} \phi_{m'+1}^S + i'_{42} \chi_4^N e^{-iq_h x} \phi_{m'}^S, & 0 < x < a/2, \\ j'_{41} \chi_3^N e^{iq_h(x-a/2)} \phi_{m'+1}^S + j'_{42} \chi_4^N e^{iq_h(x-a/2)} \phi_{m'}^S, & \\ k'_{41} \chi_1^S e^{iq_e^S x} \phi_{m'}^S + k'_{42} \chi_2^S e^{iq_e^S x} \phi_{m'+1}^S + l'_{41} \chi_3^S e^{-iq_h^S x} \phi_{m'+1}^S + l'_{42} \chi_4^S e^{-iq_h^S x} \phi_{m'}^S, & x > a/2. \end{cases}
 \end{aligned}$$

$$\begin{aligned}
\varphi_5(x) &= \begin{cases} k'_{51}\chi_1^S e^{-iq_e^S x} \phi_{m'}^S + k'_{52}\chi_2^S e^{-iq_e^S x} \phi_{m'+1}^S + l'_{51}\chi_3^S e^{iq_h^S x} \phi_{m'+1}^S + l'_{52}\chi_4^S e^{iq_h^S x} \phi_{m'}^S, & x < -a/2, \\ c'_{51}\chi_1^N e^{iq_e(x+a/2)} \phi_{m'}^S + c'_{52}\chi_2^N e^{iq_e(x+a/2)} \phi_{m'+1}^S + d'_{51}\chi_1^N e^{-iq_e x} \phi_{m'}^S + d'_{52}\chi_2^N e^{-iq_e x} \phi_{m'+1}^S + e'_{51}\chi_3^N e^{iq_h x} \phi_{m'+1}^S + e'_{52}\chi_4^N e^{iq_h x} \phi_{m'}^S, & -a/2 < x < 0, \\ g'_{51}\chi_1^N e^{-iq_e(x-a/2)} \phi_{m'}^S + g'_{52}\chi_2^N e^{-iq_e(x-a/2)} \phi_{m'+1}^S + h'_{51}\chi_1^N e^{iq_e x} \phi_{m'}^S + h'_{52}\chi_2^N e^{iq_e x} \phi_{m'+1}^S + i'_{51}\chi_3^N e^{-iq_h x} \phi_{m'+1}^S + i'_{52}\chi_4^N e^{-iq_h x} \phi_{m'}^S, & 0 < x < a/2, \\ \chi_1^{SR} e^{-iq_e^S x} \phi_{m'}^S + a'_{51}\chi_3^{SR} e^{-iq_h^S x} \phi_{m'+1}^S + a'_{52}\chi_4^{SR} e^{-iq_h^S x} \phi_{m'}^S + b'_{51}\chi_1^{SR} e^{iq_e^S x} \phi_{m'}^S + b'_{52}\chi_2^{SR} e^{iq_e^S x} \phi_{m'+1}^S, & x > a/2. \end{cases} \\
\varphi_6(x) &= \begin{cases} k'_{61}\chi_1^S e^{-iq_e^S x} \phi_{m'-1}^S + k'_{62}\chi_2^S e^{-iq_e^S x} \phi_{m'}^S + l'_{61}\chi_3^S e^{iq_h^S x} \phi_{m'}^S + l'_{62}\chi_4^S e^{iq_h^S x} \phi_{m'-1}^S, & x < -a/2, \\ c'_{61}\chi_1^N e^{iq_e(x+a/2)} \phi_{m'-1}^S + c'_{62}\chi_2^N e^{iq_e(x+a/2)} \phi_{m'}^S + d'_{61}\chi_1^N e^{-iq_e x} \phi_{m'-1}^S + d'_{62}\chi_2^N e^{-iq_e x} \phi_{m'}^S + e'_{61}\chi_3^N e^{iq_h x} \phi_{m'}^S + e'_{62}\chi_4^N e^{iq_h x} \phi_{m'-1}^S, & -a/2 < x < 0, \\ g'_{61}\chi_1^N e^{-iq_e(x-a/2)} \phi_{m'-1}^S + g'_{62}\chi_2^N e^{-iq_e(x-a/2)} \phi_{m'}^S + h'_{61}\chi_1^N e^{iq_e x} \phi_{m'-1}^S + h'_{62}\chi_2^N e^{iq_e x} \phi_{m'}^S + i'_{61}\chi_3^N e^{-iq_h x} \phi_{m'}^S + i'_{62}\chi_4^N e^{-iq_h x} \phi_{m'-1}^S, & 0 < x < a/2, \\ \chi_2^{SR} e^{-iq_e^S x} \phi_{m'}^S + a'_{61}\chi_3^{SR} e^{-iq_h^S x} \phi_{m'}^S + a'_{62}\chi_4^{SR} e^{-iq_h^S x} \phi_{m'-1}^S + b'_{61}\chi_1^{SR} e^{iq_e^S x} \phi_{m'-1}^S + b'_{62}\chi_2^{SR} e^{iq_e^S x} \phi_{m'}^S, & x > a/2. \end{cases} \\
\varphi_7(x) &= \begin{cases} k'_{71}\chi_1^S e^{-iq_e^S x} \phi_{m'-1}^S + k'_{72}\chi_2^S e^{-iq_e^S x} \phi_{m'}^S + l'_{71}\chi_3^S e^{iq_h^S x} \phi_{m'}^S + l'_{72}\chi_4^S e^{iq_h^S x} \phi_{m'-1}^S, & x < -a/2, \\ c'_{71}\chi_1^N e^{iq_e(x+a/2)} \phi_{m'-1}^S + c'_{72}\chi_2^N e^{iq_e(x+a/2)} \phi_{m'}^S + d'_{71}\chi_1^N e^{-iq_e x} \phi_{m'-1}^S + d'_{72}\chi_2^N e^{-iq_e x} \phi_{m'}^S + e'_{71}\chi_3^N e^{iq_h x} \phi_{m'}^S + e'_{72}\chi_4^N e^{iq_h x} \phi_{m'-1}^S, & -a/2 < x < 0, \\ g'_{71}\chi_1^N e^{-iq_e(x-a/2)} \phi_{m'-1}^S + g'_{72}\chi_2^N e^{-iq_e(x-a/2)} \phi_{m'}^S + h'_{71}\chi_1^N e^{iq_e x} \phi_{m'-1}^S + h'_{72}\chi_2^N e^{iq_e x} \phi_{m'}^S + i'_{71}\chi_3^N e^{-iq_h x} \phi_{m'}^S + i'_{72}\chi_4^N e^{-iq_h x} \phi_{m'-1}^S, & 0 < x < a/2, \\ \chi_3^{SR} e^{iq_h^S x} \phi_{m'}^S + b'_{71}\chi_3^{SR} e^{-iq_h^S x} \phi_{m'}^S + b'_{72}\chi_4^{SR} e^{-iq_h^S x} \phi_{m'-1}^S + a'_{71}\chi_1^{SR} e^{iq_e^S x} \phi_{m'-1}^S + a'_{72}\chi_2^{SR} e^{iq_e^S x} \phi_{m'}^S, & x > a/2. \end{cases} \\
\varphi_8(x) &= \begin{cases} k'_{81}\chi_1^S e^{-iq_e^S x} \phi_{m'}^S + k'_{82}\chi_2^S e^{-iq_e^S x} \phi_{m'+1}^S + l'_{81}\chi_3^S e^{iq_h^S x} \phi_{m'+1}^S + l'_{82}\chi_4^S e^{iq_h^S x} \phi_{m'}^S, & x < -a/2, \\ c'_{81}\chi_1^N e^{iq_e(x+a/2)} \phi_{m'}^S + c'_{82}\chi_2^N e^{iq_e(x+a/2)} \phi_{m'+1}^S + d'_{81}\chi_1^N e^{-iq_e x} \phi_{m'}^S + d'_{82}\chi_2^N e^{-iq_e x} \phi_{m'+1}^S + e'_{81}\chi_3^N e^{iq_h x} \phi_{m'+1}^S + e'_{82}\chi_4^N e^{iq_h x} \phi_{m'}^S, & -a/2 < x < 0, \\ g'_{81}\chi_1^N e^{-iq_e(x-a/2)} \phi_{m'}^S + g'_{82}\chi_2^N e^{-iq_e(x-a/2)} \phi_{m'+1}^S + h'_{81}\chi_1^N e^{iq_e x} \phi_{m'}^S + h'_{82}\chi_2^N e^{iq_e x} \phi_{m'+1}^S + i'_{81}\chi_3^N e^{-iq_h x} \phi_{m'+1}^S + i'_{82}\chi_4^N e^{-iq_h x} \phi_{m'}^S, & 0 < x < a/2, \\ \chi_4^{SR} e^{iq_h^S x} \phi_{m'}^S + b'_{81}\chi_3^{SR} e^{-iq_h^S x} \phi_{m'+1}^S + b'_{82}\chi_4^{SR} e^{-iq_h^S x} \phi_{m'}^S + a'_{81}\chi_1^{SR} e^{iq_e^S x} \phi_{m'}^S + a'_{82}\chi_2^{SR} e^{iq_e^S x} \phi_{m'+1}^S, & x > a/2. \end{cases} \tag{A2}
\end{aligned}$$

where $\chi_1^{SR} = \begin{pmatrix} ue^{i\varphi} \\ 0 \\ 0 \\ v \end{pmatrix}$, $\chi_2^{SR} = \begin{pmatrix} 0 \\ -ue^{i\varphi} \\ v \\ 0 \end{pmatrix}$, $\chi_3^{SR} = \begin{pmatrix} 0 \\ -ve^{i\varphi} \\ u \\ 0 \end{pmatrix}$ and, $\chi_4^{SR} = \begin{pmatrix} ve^{i\varphi} \\ 0 \\ 0 \\ u \end{pmatrix}$. In Eq. (A2), φ_1 , φ_2 , φ_3 ,

and φ_4 represent the wavefunctions when spin up electronlike quasiparticle, spin down electronlike quasiparticle, spin up holelike quasiparticle and spin down holelike quasiparticle are injected from left superconducting region respectively, while φ_5 , φ_6 , φ_7 , and φ_8 represent the wavefunctions when spin up electronlike quasiparticle, spin down electronlike quasiparticle, spin up holelike quasiparticle and spin down holelike quasiparticle are injected from right superconducting region respectively. The Andreev and normal reflection coefficients are a'_{mn} and b'_{mn} respectively, while the transmission coefficients for electronlike and holelike quasiparticles are k'_{mn} and l'_{mn} respectively with $m = 1, 2, \dots, 8$ and $n = 1, 2$, where $m = 1$ means spin up electronlike quasiparticle incident from left, $m = 2$ means spin down electronlike quasiparticle incident from left, $m = 3$ means spin up holelike quasiparticle incident from left, $m = 4$ means spin down holelike quasiparticle incident from left, $m = 5$ means spin up electronlike quasiparticle incident from right, $m = 6$ means spin down electronlike quasiparticle incident from right, $m = 7$ means spin up holelike quasiparticle incident from right and, finally $m = 8$ means spin down holelike quasiparticle incident from right. In a'_{mn} , $n = 1$ means spin up holelike quasiparticle reflected back to left and, $n = 2$ means spin down holelike quasiparticle reflected back to left when $m = 1, 2$, while $n = 1$ means spin up electronlike quasiparticle reflected back to left and, $n = 2$ means spin down electronlike quasiparticle reflected back to left when $m = 3, 4$. Similarly, when $m = 5, 6$, $n = 1$ means holelike quasiparticle with spin up reflected back to right and, $n = 2$ means holelike quasiparticle with spin down reflected back to right, while $n = 1$ means electronlike quasiparticle with spin up reflected back to right and, $n = 2$ means electronlike quasiparticle with spin down reflected back to right when $m = 7, 8$. In b'_{mn} , $n = 1$ means spin up electronlike quasiparticle reflected back to left and, $n = 2$ means spin down electronlike quasiparticle reflected back to left for $m = 1, 2$, while for $m = 3, 4$, $n = 1$ means spin up holelike quasiparticle reflected back to left and, $n = 2$ means spin down holelike quasiparticle reflected back to left. Further, in b'_{mn} , $n = 1$ means electronlike quasiparticle with spin up reflected back to right and, $n = 2$ means electronlike quasiparticle with spin down reflected back to right when $m = 5, 6$, while for $m = 7, 8$, $n = 1$ means holelike quasiparticle with spin up reflected back to right and, $n = 2$ means holelike quasiparticle with spin down reflected back to right. In k'_{mn} , $n = 1$ means spin up electronlike quasiparticle transmitted into right and, $n = 2$ means spin down electronlike quasiparticle transmitted into right for $m = 1, 2, 3, 4$, while $n = 1$ means spin up electronlike quasiparticle transmitted into left and, $n = 2$ means spin down electronlike quasiparticle transmitted into left for $m = 5, 6, 7, 8$. Finally, in l'_{mn} , $n = 1$ means spin up holelike quasiparticle transmitted into right and, $n = 2$ means spin down holelike quasiparticle transmitted

into right for $m = 1, 2, 3, 4$, while $n = 1$ means spin up holelike quasiparticle transmitted into left and, $n = 2$ means spin down holelike quasiparticle transmitted into left for $m = 5, 6, 7, 8$.

a. Boundary conditions for metal-spin flipper-metal-superconductor junction

From the boundary condition, we get the amplitudes in the scattering states. At $x = -a$, the boundary conditions are-

$$\varphi_i|_{x < -a} = \varphi_i|_{-a < x < 0} \text{ and, } \frac{d\varphi_i|_{-a < x < 0}}{dx} - \frac{d\varphi_i|_{x < -a}}{dx} = -\frac{2m^* \mathcal{J}_0 \vec{s} \cdot \vec{S}}{\hbar^2} \varphi_i|_{x = -a}, \quad (\text{A3})$$

where $\vec{s} \cdot \vec{S} = s^z S^z + \frac{(s^+ S^- + s^- S^+)}{2}$, $s^\pm = s_x \pm i s_y$ and $S^\pm = S_x \pm i S_y$ are the exchange operator in Hamiltonian for spin flipper[19], spin raising & lowering operators for electron and spin raising & lowering operators for spin flipper respectively. The boundary conditions at $x = 0$ are-

$$\varphi_i|_{-a < x < 0} = \varphi_i|_{x > 0} \text{ and, } \frac{d\varphi_i|_{x > 0}}{dx} - \frac{d\varphi_i|_{-a < x < 0}}{dx} = \frac{2m^* V}{\hbar^2} \varphi_i|_{x = 0}. \quad (\text{A4})$$

For wave-function associating up spin electron, action of $\vec{s} \cdot \vec{S}$ is

$$\vec{s} \cdot \vec{S} \chi_1^N \phi_{m'}^S = \frac{\hbar^2 m'}{2} \chi_1^N \phi_{m'}^S + \frac{\hbar^2 \mathcal{F}}{2} \chi_2^N \phi_{m'+1}^S. \quad (\text{A5})$$

Similarly, for wave-function associating down spin electron, action of $\vec{s} \cdot \vec{S}$ is

$$\vec{s} \cdot \vec{S} \chi_2^N \phi_{m'}^S = -\frac{\hbar^2 m'}{2} \chi_2^N \phi_{m'}^S + \frac{\hbar^2 \mathcal{F}'}{2} \chi_1^N \phi_{m'-1}^S. \quad (\text{A6})$$

Further, for wave-function associating up spin hole, action of $\vec{s} \cdot \vec{S}$ is

$$\vec{s} \cdot \vec{S} \chi_3^N \phi_{m'}^S = -\frac{\hbar^2 m'}{2} \chi_3^N \phi_{m'}^S + \frac{\hbar^2 \mathcal{F}'}{2} \chi_4^N \phi_{m'-1}^S, \quad (\text{A7})$$

and finally, for wave-function associating down spin hole, action of $\vec{s} \cdot \vec{S}$ is

$$\vec{s} \cdot \vec{S} \chi_4^N \phi_{m'}^S = \frac{\hbar^2 m'}{2} \chi_4^N \phi_{m'}^S + \frac{\hbar^2 \mathcal{F}}{2} \chi_3^N \phi_{m'+1}^S. \quad (\text{A8})$$

In Eqs. (A5)-(A8), $\mathcal{F} = \sqrt{(S - m')(S + m' + 1)}$ and $\mathcal{F}' = \sqrt{(S + m')(S - m' + 1)}$ are the flip probabilities when spin up(or, down) electron(or, hole) is incident and, when spin down (or, up) electron(or, hole) is incident respectively. After using above equations and solving boundary conditions, we will get 16 equations for each kind of incident process, see Eq. (A1). Different scattering amplitudes a_{ij} , b_{ij} , c_{ij} , d_{ij} , e_{ij} , f_{ij} , g_{ij} , h_{ij} for each kind of scattering process are obtained from these 16 equations. We use these scattering amplitudes in our main article to compute energy bound states and retarded Green's function for the setup shown in Fig. 1(a). Even/odd-frequency spin singlet and spin triplet pairings are found from retarded Green's function.

3. Boundary conditions for superconductor-metal-spin flipper-metal-superconductor junction

At $x = -a/2$, the boundary condition is-

$$\varphi_i(x < -a/2) = \varphi_i(-a/2 < x < 0), \quad (\text{A9})$$

$$\text{and, } \frac{d\varphi_i(-a/2 < x < 0)}{dx} - \frac{d\varphi_i(x < -a/2)}{dx} = \frac{2m^* V}{\hbar^2} \varphi_i(x = -a/2). \quad (\text{A10})$$

Similarly, at $x = 0$, the boundary condition is-

$$\varphi_i(-a/2 < x < 0) = \varphi_i(0 < x < a/2), \quad (\text{A11})$$

$$\text{and, } \frac{d\varphi_i(0 < x < a/2)}{dx} - \frac{d\varphi_i(-a/2 < x < 0)}{dx} = -\frac{2m^* \mathcal{J}_0 \vec{s} \cdot \vec{S}}{\hbar^2} \varphi_i(x = 0). \quad (\text{A12})$$

Finally, at $x = a/2$, the boundary condition is-

$$\varphi_i(0 < x < a/2) = \varphi_i(x > a/2), \quad (\text{A13})$$

$$\text{and, } \frac{d\varphi_i(x > a/2)}{dx} - \frac{d\varphi_i(0 < x < a/2)}{dx} = \frac{2m^*V}{\hbar^2} \varphi_i(x = a/2). \quad (\text{A14})$$

Using Eqs. (A5-A8) and solving boundary conditions at $x = -a/2$, $x = 0$ and $x = a/2$, 24 equations for each kind of incident process as mentioned in Eq. (A2) are obtained. Using these 24 equations, the various scattering amplitudes $a'_{mn}, b'_{mn}, c'_{mn}, d'_{mn}, e'_{mn}, f'_{mn}, g'_{mn}, h'_{mn}, i'_{mn}, j'_{mn}, k'_{mn}, l'_{mn}$ for each kind of scattering process can be obtained.

4. Energy bound states

To calculate energy bound states in superconductor-metal-spin flipper-metal-superconductor junction we ignore the contribution from incoming quasiparticle[29, 30] and put the wavefunction into the boundary conditions. We obtain 24 equations for the scattering amplitudes. Eliminating the scattering amplitudes of the two metals by the scattering amplitudes in the left and right superconductors we get 8 equations,

$$Lz = 0, \quad (\text{A15})$$

where z is a 8×1 column matrix and given by $z = [b_{11}, b_{12}, a_{11}, a_{12}, k_{11}, k_{12}, l_{11}, l_{12}]^T$ and L being a 8×8 matrix. For nontrivial solution of this system, the determinant of L is zero ($\det L = 0$) and we get energy bound states $E_k(\varphi)$ ($k = \{1, \dots, 4\}$) as a function of phase difference φ between right and left superconductor. We see that $E_k(\varphi) = E_\sigma^\pm(\varphi) = \pm E_\sigma(\varphi)$, ($\sigma = \uparrow, \downarrow$).

5. Retarded and Advanced Green's functions in presence of YSR bound states

The main aim of our work is to check whether presence of YSR bound states and the occurrence of odd ω pairing have any relation or not. To this end we construct retarded Green's function $G^r(x, x', \omega)$ for our setups shown in Figs. 1(a) & (b) from the scattering processes at the interface[26]. We follow Refs. 27 and 28 and the retarded Green's function is given as-

$$G^r(x, x', \omega) = \begin{cases} \begin{aligned} &\varphi_1(x)[\alpha_{11}\tilde{\varphi}_5^T(x') + \alpha_{12}\tilde{\varphi}_6^T(x') + \alpha_{13}\tilde{\varphi}_7^T(x') + \alpha_{14}\tilde{\varphi}_8^T(x')] \\ &+ \varphi_2(x)[\alpha_{21}\tilde{\varphi}_5^T(x') + \alpha_{22}\tilde{\varphi}_6^T(x') + \alpha_{23}\tilde{\varphi}_7^T(x') + \alpha_{24}\tilde{\varphi}_8^T(x')] \\ &+ \varphi_3(x)[\alpha_{31}\tilde{\varphi}_5^T(x') + \alpha_{32}\tilde{\varphi}_6^T(x') + \alpha_{33}\tilde{\varphi}_7^T(x') + \alpha_{34}\tilde{\varphi}_8^T(x')] \\ &+ \varphi_4(x)[\alpha_{41}\tilde{\varphi}_5^T(x') + \alpha_{42}\tilde{\varphi}_6^T(x') + \alpha_{43}\tilde{\varphi}_7^T(x') + \alpha_{44}\tilde{\varphi}_8^T(x')] \end{aligned} & x > x' \\ \begin{aligned} &\varphi_5(x)[\beta_{11}\tilde{\varphi}_1^T(x') + \beta_{12}\tilde{\varphi}_2^T(x') + \beta_{13}\tilde{\varphi}_3^T(x') + \beta_{14}\tilde{\varphi}_4^T(x')] \\ &+ \varphi_6(x)[\beta_{21}\tilde{\varphi}_1^T(x') + \beta_{22}\tilde{\varphi}_2^T(x') + \beta_{23}\tilde{\varphi}_3^T(x') + \beta_{24}\tilde{\varphi}_4^T(x')] \\ &+ \varphi_7(x)[\beta_{31}\tilde{\varphi}_1^T(x') + \beta_{32}\tilde{\varphi}_2^T(x') + \beta_{33}\tilde{\varphi}_3^T(x') + \beta_{34}\tilde{\varphi}_4^T(x')] \\ &+ \varphi_8(x)[\beta_{41}\tilde{\varphi}_1^T(x') + \beta_{42}\tilde{\varphi}_2^T(x') + \beta_{43}\tilde{\varphi}_3^T(x') + \beta_{44}\tilde{\varphi}_4^T(x')] \end{aligned} & x < x' \end{cases} \quad (\text{A16})$$

In Eq. (A16), α_{ij} and β_{mn} are computed from the continuity of the Green's function

$$[\omega - H_{BdG}(x)]G^r(x, x', \omega) = \delta(x - x'), \quad (\text{A17})$$

After integrating Eq. A17 around $x = x'$ we find

$$[G^r(x > x')]_{x=x'} = [G^r(x < x')]_{x=x'} \text{ and } \left[\frac{d}{dx}G^r(x > x')\right]_{x=x'} - \left[\frac{d}{dx}G^r(x < x')\right]_{x=x'} = \eta\tau_z\sigma_0, \quad (\text{A18})$$

where τ_i represent Pauli matrices in particle-hole space, while σ_i represent Pauli matrices in spin space and, $\eta = 2m^*/\hbar^2$. Generally, in particle-hole space G^r is a 2×2 matrix,

$$G^r(x, x', \omega) = \begin{bmatrix} G_{ee}^r & G_{eh}^r \\ G_{he}^r & G_{hh}^r \end{bmatrix}, \quad (\text{A19})$$

where $G_{ee}^r, G_{eh}^r, G_{he}^r$ are matrix. In presence of spin flip scattering, we can write each element of $G^r(x, x', \omega)$ as

$$G_{ab}^r(x, x', \omega) = \begin{pmatrix} [G_{ab}^r]_{\uparrow\uparrow} & [G_{ab}^r]_{\uparrow\downarrow} \\ [G_{ab}^r]_{\downarrow\uparrow} & [G_{ab}^r]_{\downarrow\downarrow} \end{pmatrix}, \text{ with } a, b \in \{e, h\}. \quad (\text{A20})$$

The next section provides an explicit form of Green's functions.

6. Explicit form of expressions for Anomalous Green's functions

Here, we give an explicit form of expressions for anomalous Green's functions (G_{eh}^r). We compute SS and ST pairing in our main article using G_{eh}^r .

a. Metal (N_1)-Spin flipper (sf)-Metal (N_2)-Superconductor (S) junction

In case of N_1 -sf- N_2 -S junction, G^r are determined by putting wavefunctions from Eq. (A1) into Eq. (A16) with a_{ij} and b_{ij} found from Eqs. (A3)-(A4). For G_{eh}^r we get,

$$\begin{aligned} [G_{eh}^r]_{\uparrow\uparrow} &= -[G_{eh}^r]_{\downarrow\downarrow} = -\frac{\eta}{2i(u^2 - v^2)} \left[\frac{b_{61} e^{iq_e^S(x+x')} uv + a_{62} e^{i(q_e^S x' - q_h^S x)} v^2}{q_e^S} + \frac{a_{62} e^{i(q_e^S x - q_h^S x')} u^2 - b_{72} e^{-iq_h^S(x+x')} uv}{q_h^S} \right], \\ [G_{eh}^r]_{\uparrow\downarrow} &= -[G_{eh}^r]_{\downarrow\uparrow} = \frac{\eta}{2i(u^2 - v^2)} \left[\frac{e^{iq_e^S|x-x'|} uv + b_{51} e^{iq_e^S(x+x')} uv + a_{81} e^{i(q_e^S x' - q_h^S x)} v^2}{q_e^S} \right. \\ &\quad \left. + \frac{a_{81} e^{i(q_e^S x - q_h^S x')} u^2 + b_{82} e^{-iq_h^S(x+x')} uv + e^{-iq_h^S|x-x'|} uv}{q_h^S} \right]. \end{aligned} \quad (A21)$$

b. Superconductor (S)-Metal (N_1)-Spin flipper (sf)-Metal (N_2)-Superconductor (S) junction

In case of S- N_1 -sf- N_2 -S junction, G^r are obtained by putting wavefunctions from Eq. (A2) into Eq. (A16) with a'_{ij} and b'_{ij} found from Eqs. (A9)-(A14). For G_{eh}^r we get

$$\begin{aligned} [G_{eh}^r]_{\uparrow\uparrow} &= -[G_{eh}^r]_{\downarrow\downarrow} = -\frac{\eta}{2i(u^2 - v^2)} \left[\frac{b'_{21} e^{-iq_e^S(x+x')} uv + a'_{22} e^{-i(q_e^S x' - q_h^S x)} v^2}{q_e^S} - \frac{a'_{31} e^{-i(q_e^S x - q_h^S x')} u^2 + b'_{32} e^{iq_h^S(x+x')} uv}{q_h^S} \right], \\ [G_{eh}^r]_{\uparrow\downarrow} &= -[G_{eh}^r]_{\downarrow\uparrow} = \frac{\eta}{2i(u^2 - v^2)} \left[\frac{e^{iq_e^S|x-x'|} uv + b'_{11} e^{-iq_e^S(x+x')} uv + a'_{12} e^{-i(q_e^S x' - q_h^S x)} v^2}{q_e^S} \right. \\ &\quad \left. + \frac{a'_{41} e^{-i(q_e^S x - q_h^S x')} u^2 + b'_{42} e^{iq_h^S(x+x')} uv + e^{-iq_h^S|x-x'|} uv}{q_h^S} \right]. \end{aligned} \quad (A22)$$